Phospholipid headgroup composition modulates the molecular interactions and antimicrobial effects of sulfobetaine zwitterionic detergents against the “ESKAPE” pathogen *Pseudomonas aeruginosa*.†

Kira L. F. Hilton,[a] Howard Tolley,[b] Jose L. Ortega-Roldan,[a] Gary S. Thompson,[a] J. Mark Sutton,[b,c] Charlotte K. Hind,[b*] and Jennifer R. Hiscock.[a*]

[a] Division of Natural Sciences, University of Kent, Canterbury, CT2 7NH, UK. Email; J.R.Hiscock@Kent.ac.uk
[b] UKHSA, Science Group, Manor Farm Road, Salisbury. SP4 0JG; Email: charlotte.hind@ukhsa.gov.uk
[c] Institute of Pharmaceutical Sciences, School of Cancer & Pharmaceutical Sciences King’s College London, SE1 9NQ

Contents

Section 1: Chemical structures

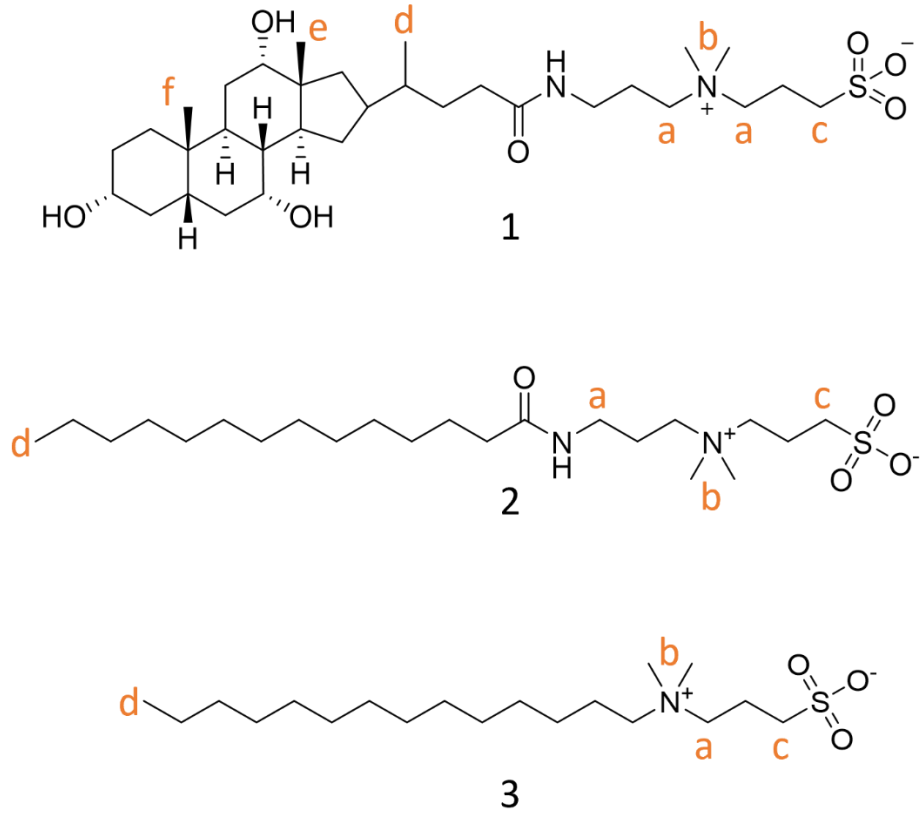

Figure S1 – Chemical structure of **1** (CHAPS), **2** (ASB-14) and **3** (SB 3-14), with the proton environments for ^{1}H NMR resonances labelled in orange. The same letters have been used for different proton environments where the ^{1}H NMR resonances have been found to overlap.

Section 2: Experimental

General remarks: The NMR spectra were obtained using an Avance III 600 Hz spectrometer and processed using processed MestreNova software. Compounds **1** - **3** were purchased from commercial sources with a purity level of ≥ 95 % confirmed by HPLC analysis.

DLS potential studies: All vials used for preparing samples were clean and dry. Milli-Q® water was filtered to remove any particulates that may interfere with the results obtained. Samples were heated to ~50 ˚C and then filtered also to remove any potential solid beads from synthesis. A of 9 or 10 runs were recorded at 25 ˚C, allowing 10 mins for sample equilibration before the first measurement was recorded. These data were then averaged.

Phospholipid extraction: Bacterial cells were grown to stationary phase in 500mL tryptic soy broth (TSB), pelleted through centrifugation and resuspended in small volumes of TSB. The cells were then boiled at 98°C for 30 minutes and then snap frozen and stored at -80 to result in non-viable cells. The preparations were resuspended in Lysis buffer (300 mM NaCl, 50 mM NaH_2PO_4), then sonicated for a total time of 10 minutes, alternated on/off 30 s at a time. The preparations were centrifuged at 10,000 rpm at 4 ˚C for 15 minutes. The resultant supernatant was then centrifuged at 40,000 rpm at 4 ˚C for 1 hour. Membrane pellet resuspended in 1 mL Lysis buffer and extracted using the Folch method.[1] Briefly, methanol (7.5 mL) was added to the suspension and mixed, chloroform (15 mL) added and incubated for 1 hour at 25 ˚C. Phase separation induced by the addition of water (6.25 mL), after 1 hour at 25 ˚C, the lower layer was collected and dried.

Nanodisc preparation: Lipid films were resuspended in Buffer A (20 mM NaCl, 20 mM NaH_2PO_4, pH 7.4) and sonicated for 1 hour, at a 5:1 ratio, SMA was added and incubated at 37 ˚C for 1 hour. Dialysed overnight in 5 L of the same buffer in 10 KDa cut-off dialysis tubing, concentrated, and underwent gel filtration size exclusion chromatography on a Superdex 200 10/300 GL column (GE Healthcare) in the same buffer, whilst monitoring absorbance at 260 nm. Nanodisc quantification carried out via monitoring of absorbance at 260 nm using a calibration curve.[2] Nanodiscs to be stored for future use were aliquoted into 50 µM in 100 µL portions and stored at -80 °C.

Preparing ^{1}H NMR titration solutions: Firstly Solution A was prepared. Solution A: **1** - **3** (56 µL of a 5mM stock solution in Buffer A – see nanodisc preparation), 4,4-dimethyl4-silapentane-1-sulfonic acid (DSS - 28 µL, 2 mM stock), D2O (112 µL) and Buffer A (2604 µL). Twelve 200 µL portions of Solution A was aliquoted into eppendorf's, where differing ratios of nanodisc/buffer A were added (0.26 µM - 3.91 µM of nanodisc). The solutions in the eppendorf's were transferred to 3 mm 600 MHz NMR tubes using 1 mm teflon tubing and a blunt needle.

^{1}H NMR CPMG: ^{1}H NMR CPMG[3,4] spectra were obtained with a Bruker Avance III 600 MHz spectrometer equipped with a QCI-P cryoprobe at 298 K. Samples were supplemented with 5 % D_2O for locking and DSS (0.02 mM) as a chemical shift standard. The standard zgprcpmg pulse sequence from the Bruker library was modified with a watergate element to allow suppression of the water signal and was used for all experiments. This sequence is available on request from the authors. Presaturation was applied between acquisitions for 100 ms at a power level of 1.78×10^{-5} W, further water suppression was achieved with a 3-9-19 watergate sequence using 1 ms gradient pulses with a smoothed chirp shape and a peak Z gradient field strength of 21.2 G. The CPMG element had a length of 300 ms with delays between 180 ^{o} pulses of 1 ms. Repetition times were chosen to achieve suitable water suppression (RG < 256) with the presat and watergate sequences used with the 95 % H_2O : 5 % D_2O solvent. The length of the CPMG element was chosen to achieve good differentiation between unbound and strongly bound ligands. Data was collected with 16,384

points and a spectral width of 16.0242 ppm, the receiver gain was set to 256, with 512 scans, 8 dummy scans were acquired with an interscan delay. Data was processed using MestreNova version 14.2.2. All spectra were automatically phased and baselined corrected and chemical shifts were calibrated to the centre of the DSS peak.

Processing titration data: The NMR resonances of interest were integrated to give the 'absolute area'. These data were then data was normalised and converted to percentage co-ordination. These data were then fitted to Hill Plot Kinetics: growth/sigmoidal category, Hill function, Levenberg Marquardt iteration algorithm. V_{max} was fixed to 100 % as this was the greatest proportion of **1** - **3** that could be coordinated to the nanodiscs. Normalising - All absolute integration values was divided by the initial titration point (0 mM of nanodisc) to give values ranging from 0 - 1.

2D NMR sample preparation: All samples were prepared in solvent mixture A (75 % $CDCl_3$, 25 % MeOD, 0.032 M TMP). Samples contained 1-3 mg of lipid dissolved in ~600 µL of solvent mixture A.

2D NMR Experiments: ^{1}H-^{31}P HSQC NMR spectra were acquired on a Bruker Avance III 600 MHz spectrometer using a QCIP cryoprobe with a standard ^{31}P pre-amplifier without enhanced sensitivity from cryogenic cooling. Initial 1D ^{1}H experiment were measured for quality control. Spectra were acquired using the pulse sequence na_hsqcetf3gpxy.[5] Time domain data of 2048 and 128 complex points were used in the direct and indirect domains respectively. The sweep widths used in the ^{1}H and ^{31}P dimensions were 14423 and 2915 Hz respectively. The inter scan delay was set to 1 s and 256 scans were acquired per increment with 16 dummy scans at the start of each experiment. Offsets of 4.70 and -1.00 ppm were used for the ^{1}H and ^{31}P channels. ^{1}H decoupling was achieved during acquisition using a GARP4 sequence and the CPMG sequence during the ^{1}H-^{31}P/ ^{31}P-^{1}H transfers used 256 loops, and delays of 215 µs. The gain was limited to a maximum of 256. 2D spectra were processed with MestReNova version 14.2.2. All 2D NMR spectra were automatically phased and chemical shifts were calibrated to the centre of the TMP peak (^{1}H = 3.78 ppm, ^{31}P = 2.07 ppm).

Lipid quantification: Quantification of lipids was carried out using the 2D HSQC ^{1}H-^{31}P NMR spectra. The relevant 2D peak was picked and the percentage of total phospholipid in each sample is calculated using the ratio of each phospholipid intensity over the sum of the intensities of all phospholipids.

Preparation of DPH labelled vesicles: Lipid films were resuspended in Buffer B (150 mM KCl, 10 mM HEPES, pH 7.4, 2 mM EGTA) and subjected to 9 freeze-thaw cycles in liquid nitrogen and extruded 20 times through a 200 nm polycarbonate membrane. For fluorescent labelling, the desired vesicles were pre-incubated with 1,6-diphenyl-hexa-1,3,5-triene (DPH) (10 µM) at 60 °C for 1 hour.

Membrane fluidity assay: Black bottom 96-well plates were prepared by serially diluting desired compound in H_2O across the plate, the appropriate DPH labelled vesicles (100 µL, 30 µM) were added to each well to give a total well volume of 200 µL. FP measurements were taken at 25 °C using a 355 nm filter for excitation and a 430 m for emission. The DPH labelled vesicles were set to a FP value of 100 mP. Data were acquired in endpoint mode. All experiments were repeated in triplicate to ensure experimental reproducibility.

Section 3: Microbial materials and methods

General remarks: Bacterial strains were maintained on Tryptic Soy Agar and all assays were carried out in cation-adjusted Mueller Hinton Broth (MHB) unless otherwise stated.

Minimum Inhibitory Concentrations (MICs): MICs, defined as the lowest concentration of compound need to inhibit 100 % of visible bacterial growth. MIC_{50} defined as the lowest concentration of compound needed to inhibit 50 % of visible bacterial growth. Both values were determined experimentally using broth microdilution methods. Briefly, compounds were added to the first column of a 96 well plate and serially diluted down the plate in MH. Bacteria were added to the plate at a final concentration of 5×10^6 CFU/mL. Media only controls and untreated bacterial controls were included. Plates were incubated at 37 °C for 20 hours in a CLARIOstar plate reader (BMG Labtech) and the OD600 was read every hour.

Scanning electron microscopy: Bacteria were treated with compounds at 1 mM and 32 mM for 24 hours before being fixed using formaldehyde. Bacteria were then immobilised on poly-l-lysine coated 10mm diameter glass coverslips overnight in a humid chamber at room temperature. Samples on coverslips were secondarily fixed in 2 % osmium tetroxide for 1 hour at room temperature. Coverslips were then dehydrated through a graded ethanol series at room temperature, washed twice in hexamethyldisilazane (HDMS), then air dried. Coverslips were attached to SEM stubs using adhesive carbon disc and gold coated using Atom Tech Ultra Fine Grain Sputter Coater (Z705) and examined using a Zeiss Sigma 300VP SEM.

NPN assay: NPN assay: 1-*N*-phenylnaphtylamine (NPN) is a fluorescent probe which is excluded from the outer membrane due to its hydrophobic nature. When the outer membrane is damaged, NPN can enter into the phospholipid layer, resulting in prominent fluorescence.[6] Bacteria in mid-logarithmic growth were washed twice in buffer A (5 mM HEPES buffer, 5 mM glucose, pH 7.2) and added to a black 96 well plate containing compounds dilutions and the positive control polymyxin b at 10 µg/mL. NPN was added at a final concentration of 10 µM immediately before fluorescence was measured (350ex, 420em) using a CLARIOstar plate reader. The outer membrane permeabilization was calculated as follows: Outer membrane permeabilization (%) = $(F_{0bs} - F_0) / (F_{100} - F_0) \times 100\%$, where F_{0bs} is the observed fluorescence of the sample, F_0 is the initial fluorescence of NPN in bacteria in the absence of compound, and F_{100} is the fluorescence of NPN with bacteria upon the addition of 100 mM CHAPs.

Section 4: Summary data Tables

Table S1 – Summary table of physicochemical studies from literature and experimentally derived. Size calculated using dynamic light scattering (DLS). Experimental data carried out at 10 mM.

	Literature		**Experimental**			
	Size (nm)	CAC (mM)	DLS data			
			Size 1 (nm)	Size 2 (nm)	Size 3 (nm)	PDI (%)
1	*a*	6.4[7]	3.3	27.0	47.5	26.3
2	5.0[8]	0.1[9]	6.6	*b*	*b*	8.2
3	2.7[10]	0.4[10]	5.8	586.6	*b*	26.3

a – Data not found.

b – Primary peak only.

Table S2 - R^2, Hill coefficient and EC_{50} (μM) values obtained from the fitting of nanodisc titration data to Hill Plot kinetics using Origin 2022 software, with V_{max} fixed to 100 % of **1** bound to the nanodiscs. Data is ranked, with 1 = ^{1}H resonance with lowest EC_{50} value.

1	**PAO1**				**NCTC 13437**			
	R^2	**Hill coefficient**	**EC_{50}**	**Ranked**	**R^2**	**Hill coefficient**	**EC_{50}**	**Ranked**
a	n/a	n/a	n/a	n/a	n/a	n/a	n/a	n/a
b	0.981	1.650	3.365	4	n/a	n/a	n/a	n/a
c	n/a	n/a	n/a	n/a	n/a	n/a	n/a	n/a
d	0.995	2.207	0.633	3	0.990	1.954	0.815	3
e	0.996	1.919	0.575	1	0.994	1.675	0.689	1
f	0.994	2.042	0.581	2	0.992	1.770	0.717	2

n/a – Where 50 % co-ordination not reached, data not fitted.

Table S3 - R^2, Hill coefficient and EC_{50} (μM) values obtained from the fitting of nanodisc titration data to Hill Plot kinetics using Origin 2022 software, with V_{max} fixed to 100 % of **2** bound to the nanodiscs. Data is ranked, with 1 = ^{1}H resonance with lowest EC_{50} value.

2	**PAO1**				**NCTC 13437**			
	R^2	**Hill coefficient**	**EC_{50}**	**Ranked**	**R^2**	**Hill coefficient**	**EC_{50}**	**Ranked**
a	0.964	0.733	0.317	3	0.970	2.616	0.524	3
b	0.980	1.487	0.240	1	0.988	2.084	0.228	1
c	0.923	1.458	0.791	4	0.997	1.787	1.082	4
d	0.960	1.259	0.269	2	0.978	1.143	0.329	2

Table S4 - R^2, Hill coefficient and EC_{50} (μM) values obtained from the fitting of nanodisc titration data to Hill Plot kinetics using Origin 2022 software, with V_{max} fixed to 100 % of **3** bound to the nanodiscs. Data is ranked, with 1 = ^{1}H resonance with lowest EC_{50} value.

3	**PAO1**				**NCTC 13437**			
	R^2	**Hill coefficient**	**EC_{50}**	**Ranked**	**R^2**	**Hill coefficient**	**EC_{50}**	**Ranked**
a	0.970	1.851	0.313	3	0.995	2.121	0.189	2
b	0.998	2.269	0.193	1	0.999	2.348	0.143	1
c	0.989	1.455	0.504	4	0.998	1.625	0.319	4
d	0.998	2.404	0.222	2	0.998	2.296	0.214	3

Section 5: Dynamic light scattering data (DLS)

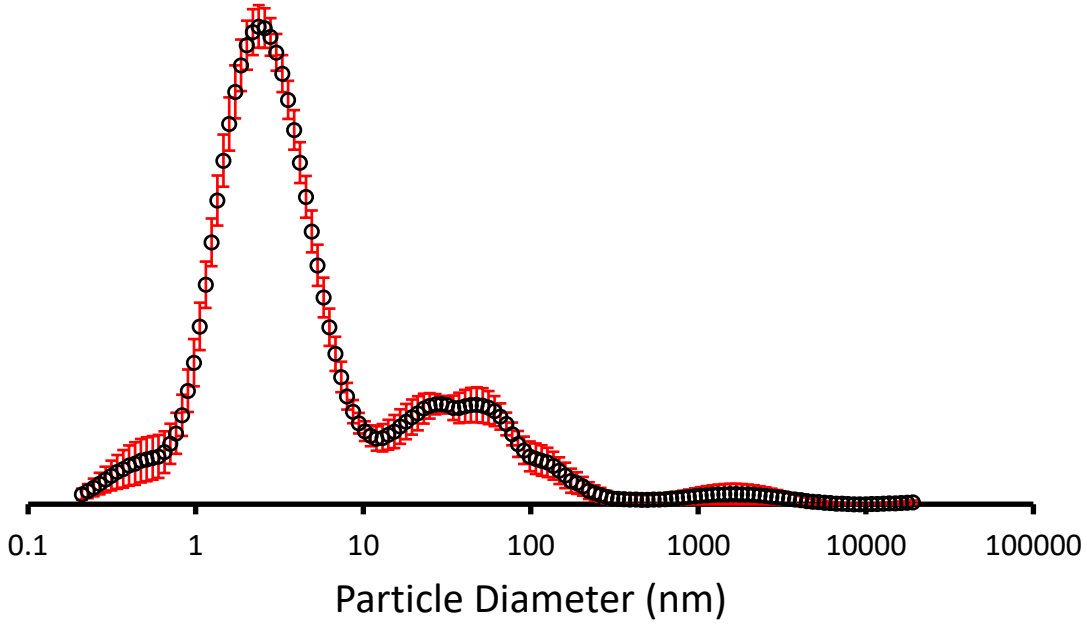

Figure S2 - The average intensity particle size distribution calculated (26 nm) using 10 DLS runs for compound **1** (10.0 mM) in an EtOH:H_2O (1:19) solution at 298 K.

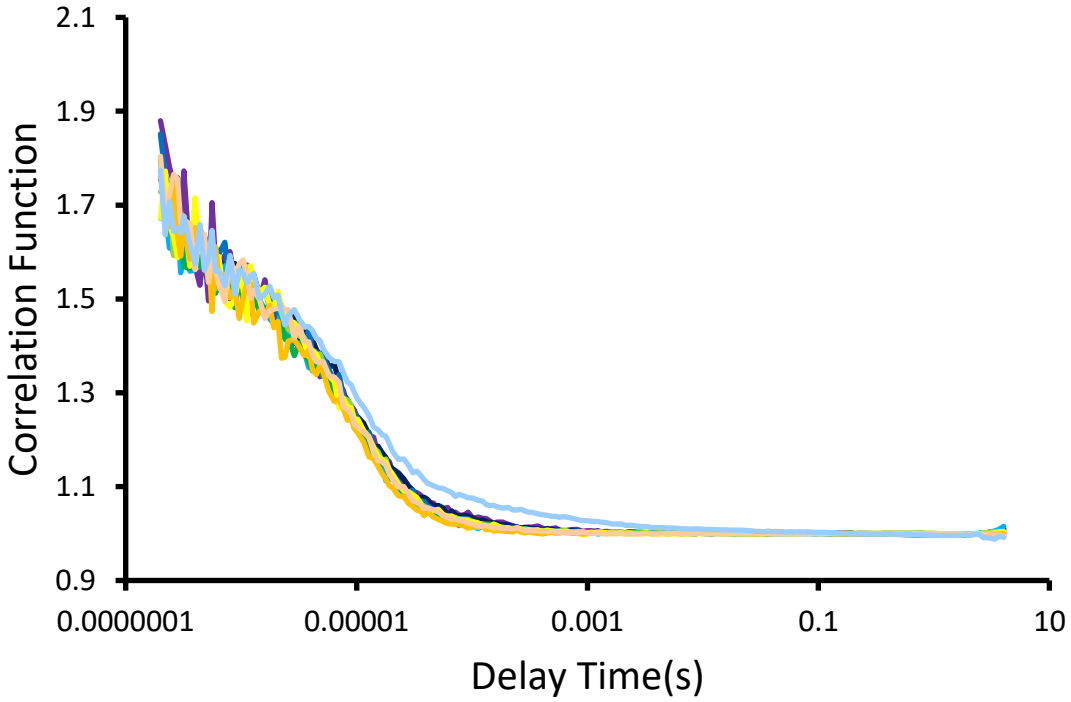

Figure S3 - Correlation function data for 10 DLS runs of compound **1** (10.0 mM) in an EtOH:H_2O (1:19) solution at 298 K.

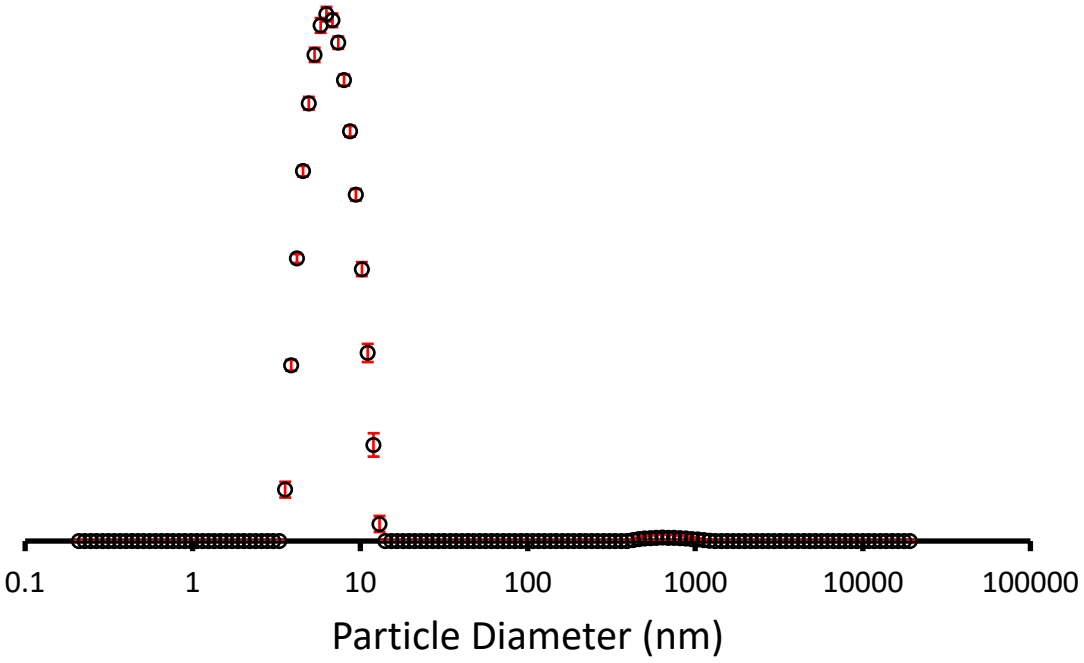

Figure S4 - The average intensity particle size distribution calculated (6.6 nm) using 10 DLS runs for compound **2** (10.0 mM) in an EtOH:H_2O (1:19) solution at 298 K.

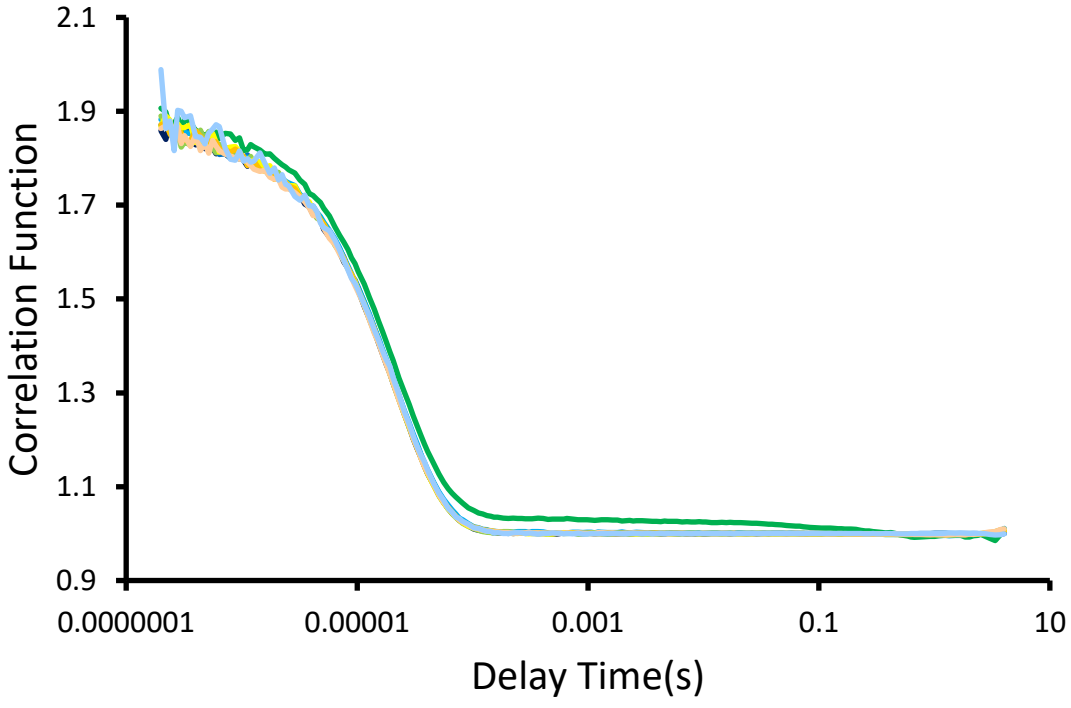

Figure S5 - Correlation function data for 10 DLS runs of compound **2** (10.0 mM) in an EtOH:H_2O (1:19) solution at 298 K.

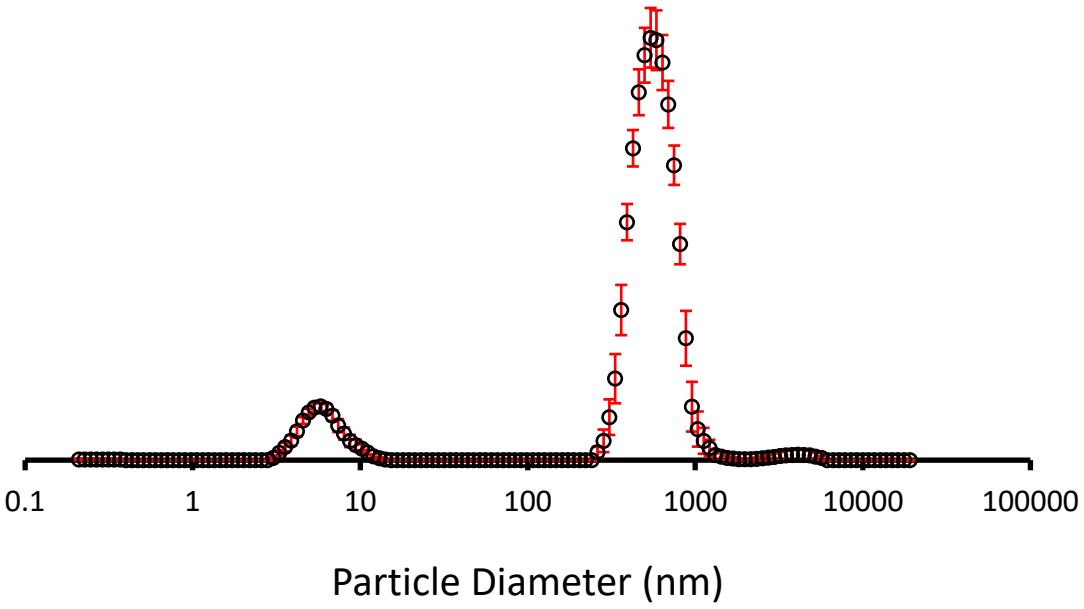

Figure S6 - The average intensity particle size distribution calculated (5.6, 586.6 nm) using 10 DLS runs for compound **3** (10.0 mM) in an EtOH:H_2O (1:19) solution at 298 K.

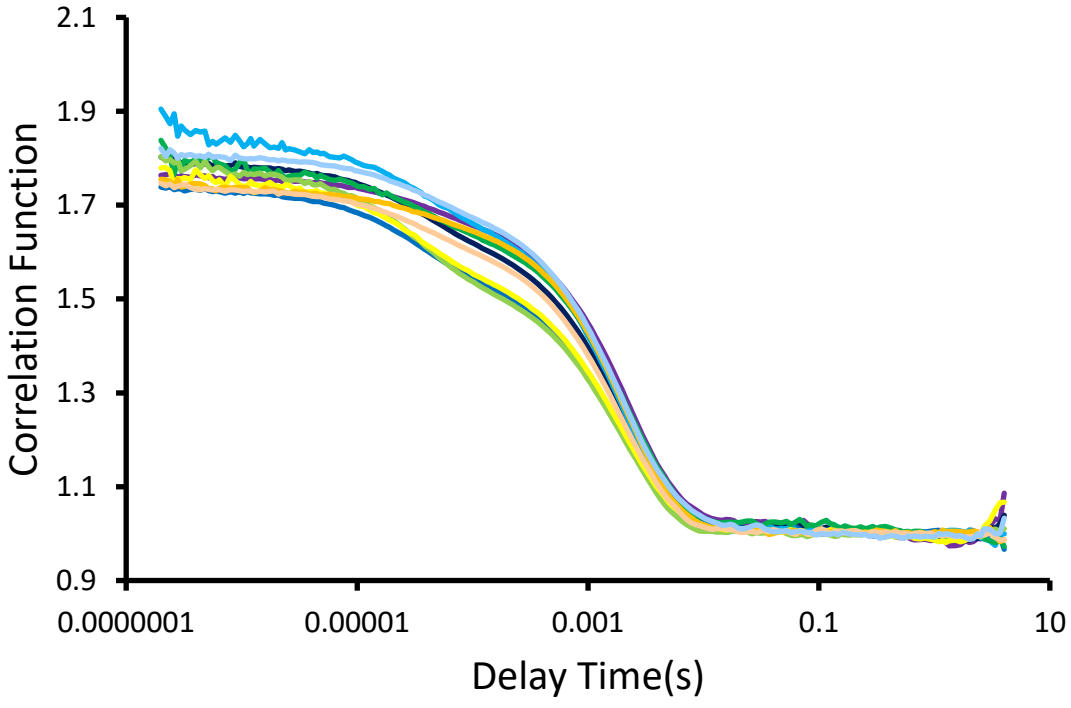

Figure S7 - Correlation function data for 10 DLS runs of compound **3** (10.0 mM) in an EtOH:H_2O (1:19) solution at 298 K.

Section 6: $^{1}H/^{31}P$ 2D NMR phospholipid head group characterisation

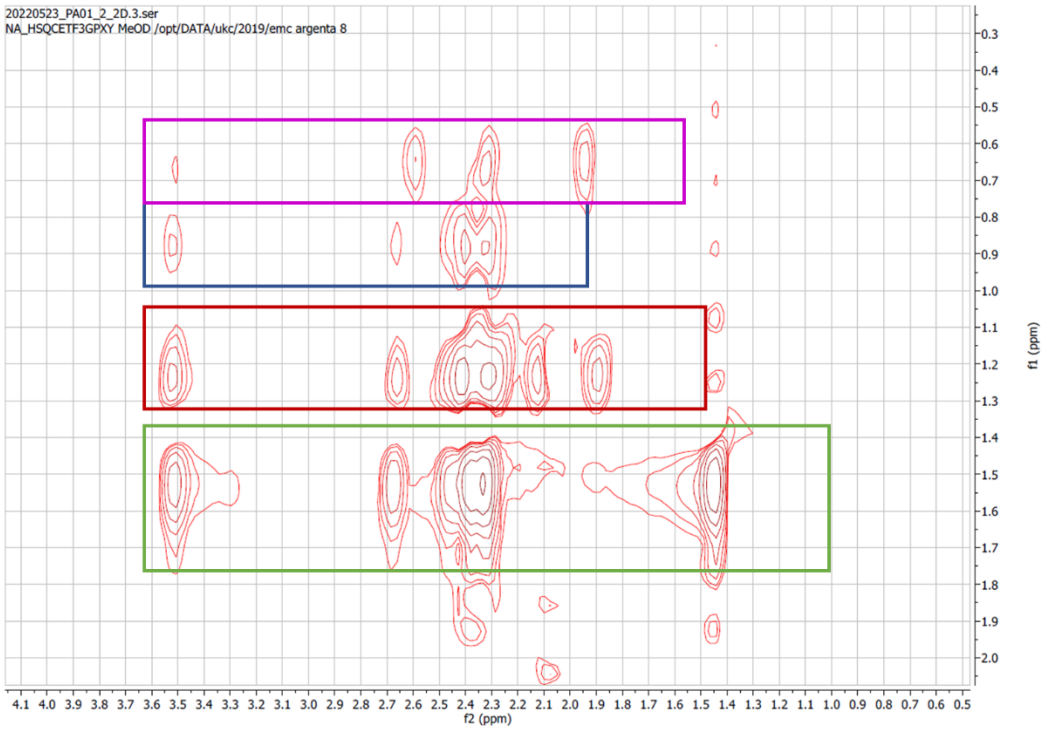

Figure S8 - 2D ^{1}H-^{31}P HSQC NMR spectrum of PAO1 lipids in solvent mixture A. Purple = PS, 2.7 %, blue = PI, 4.3 %, red = PG, 19.9 %, green = PE 73.1 %.

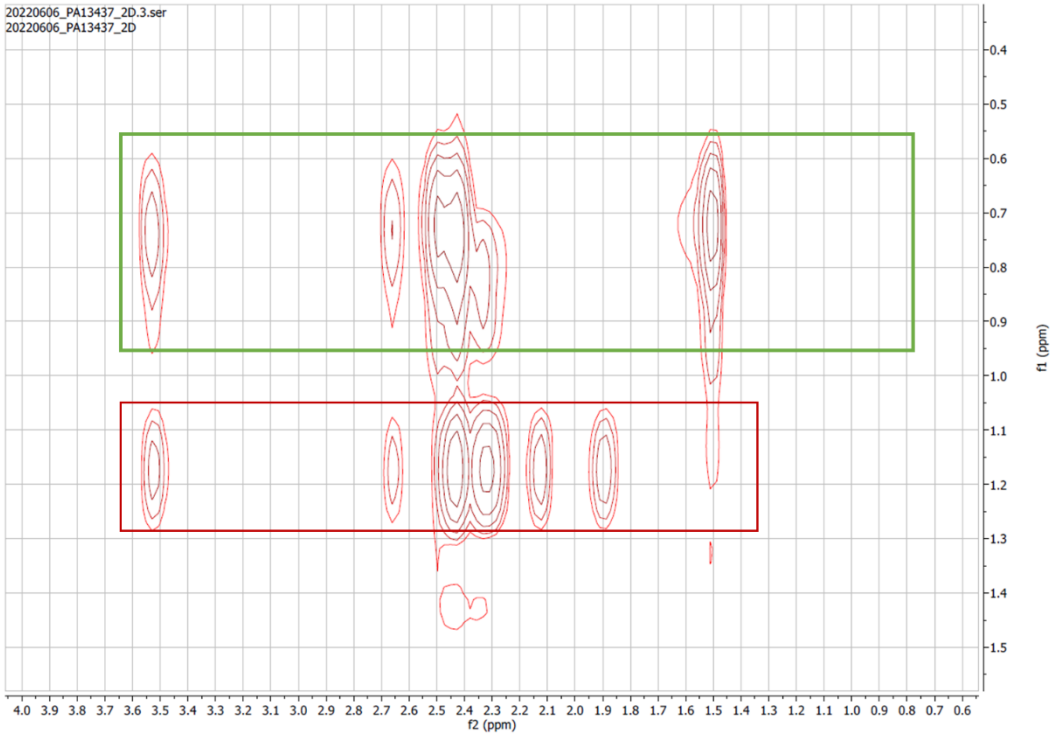

Figure S9 - 2D ^{1}H-^{31}P HSQC NMR spectrum of NCTC 13437 lipids in solvent mixture A. Green = PE, 53.4 %, red = PG, 46.6 %.

Section 7: Nanodisc characterisation data

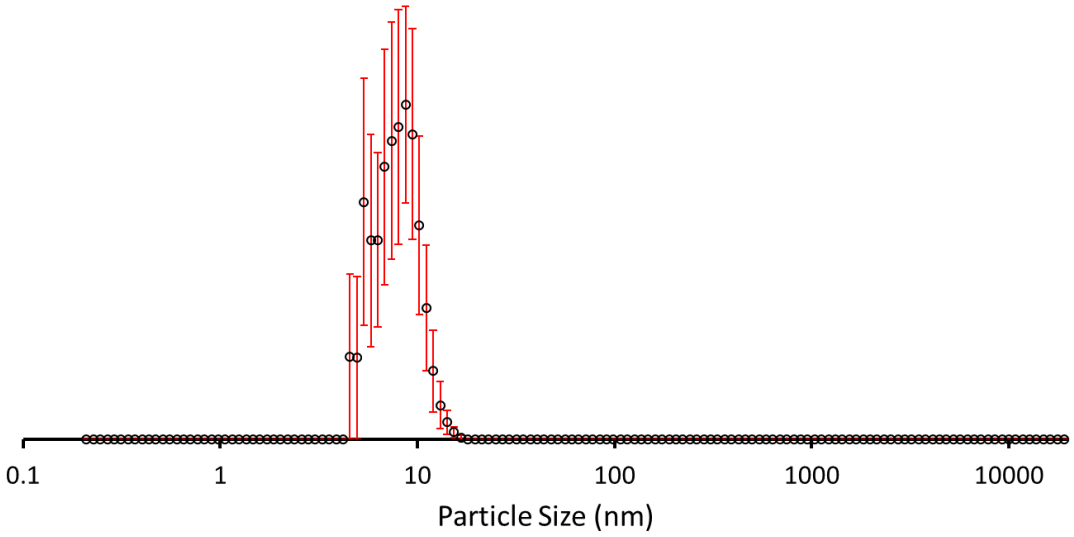

Figure S10 - Average number weighted particle size distribution of PE:PG 3:1 mix nanodiscs (100 μmols) in buffer (NaCl 20 mM, NaH_2PO_4 20 mM, pH 7.4), calculated from 10 DLS runs at 298 K.

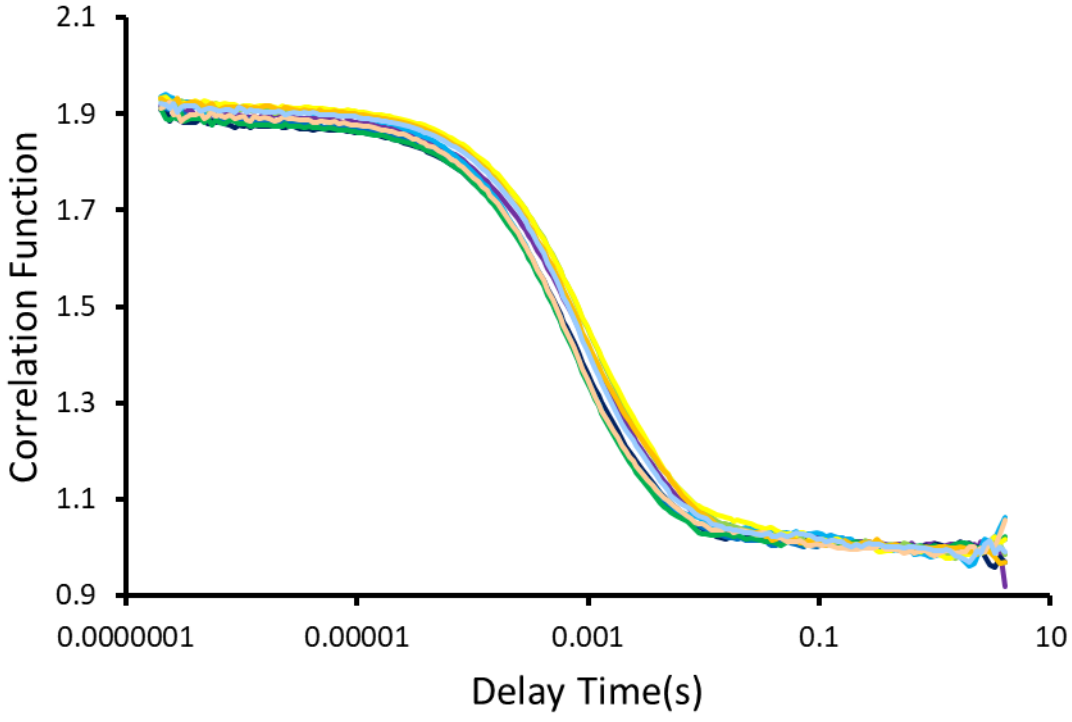

Figure S11 - Correlation function data for 9 DLS runs of NCTC 13437 nanodiscs (100 μmols) in buffer (NaCl 20 mM, NaH_2PO_4 20 mM, pH 7.4) at 298 K.

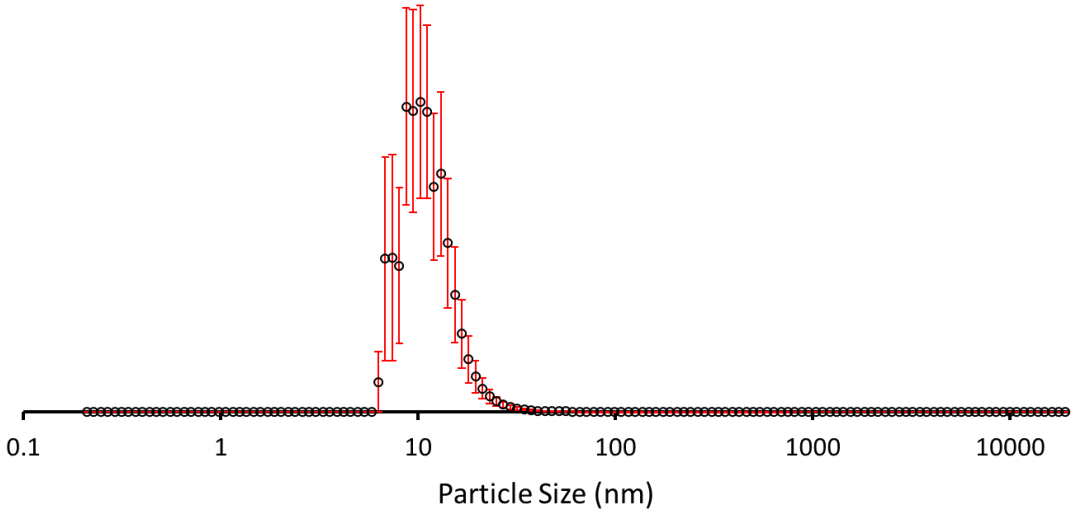

Figure S12 - Average number weighted particle size distribution of NCTC 13437 nanodiscs (100 μmols) in buffer (NaCl 20 mM, NaH_2PO_4 20 mM, pH 7.4), calculated from 10 DLS runs at 298 K.

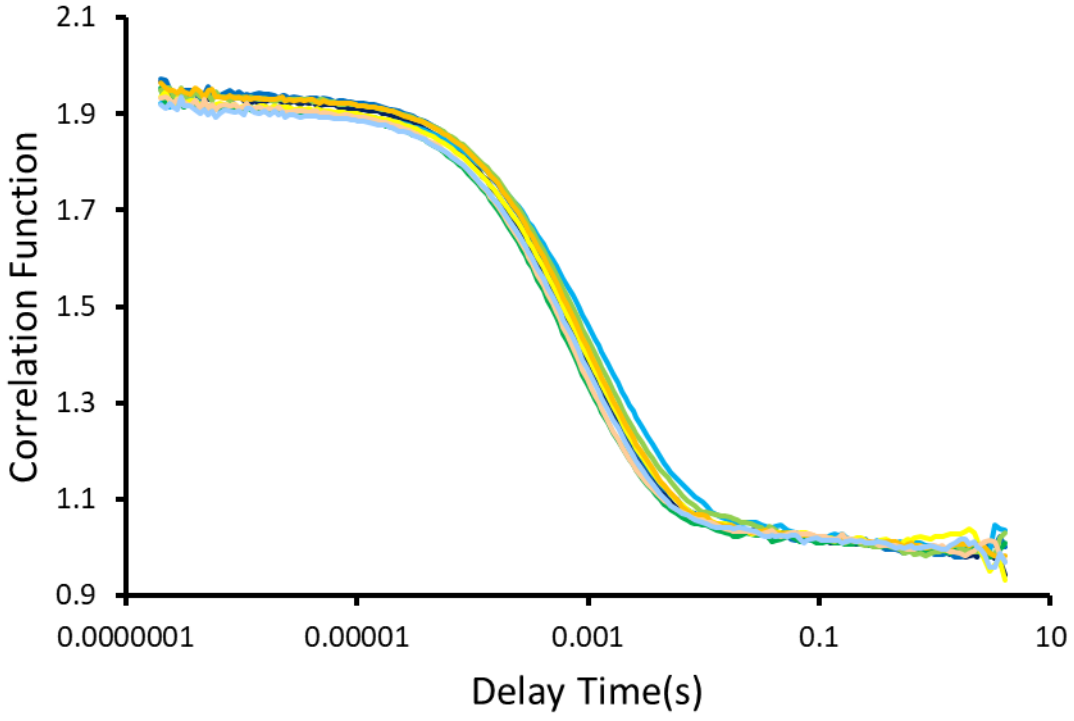

Figure S13 - Correlation function data for 9 DLS runs of NCTC 13437 nanodiscs (100 μmols) in buffer (NaCl 20 mM, NaH_2PO_4 20 mM, pH 7.4) at 298 K.

Section 8: CPMG ^{1}H NMR titration data

Raw ^{1}H NMR titration data

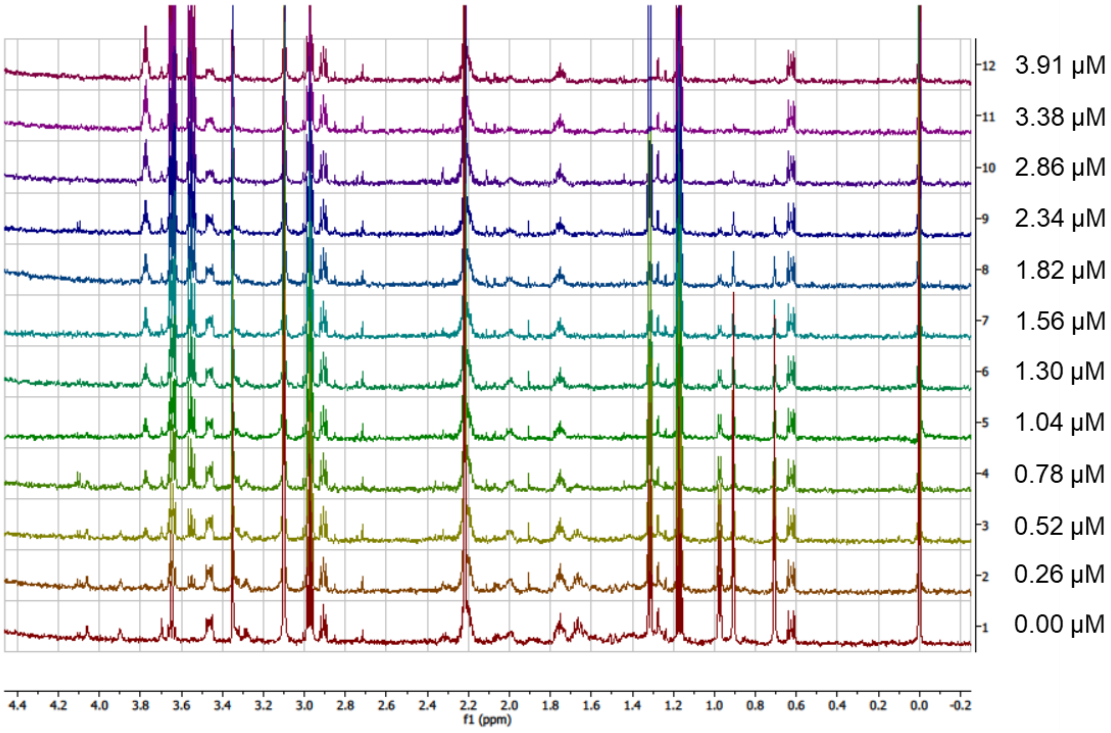

Figure S14 - Raw ^{1}H NMR titration data of **1** against PAO1 nanodiscs, n = 1.

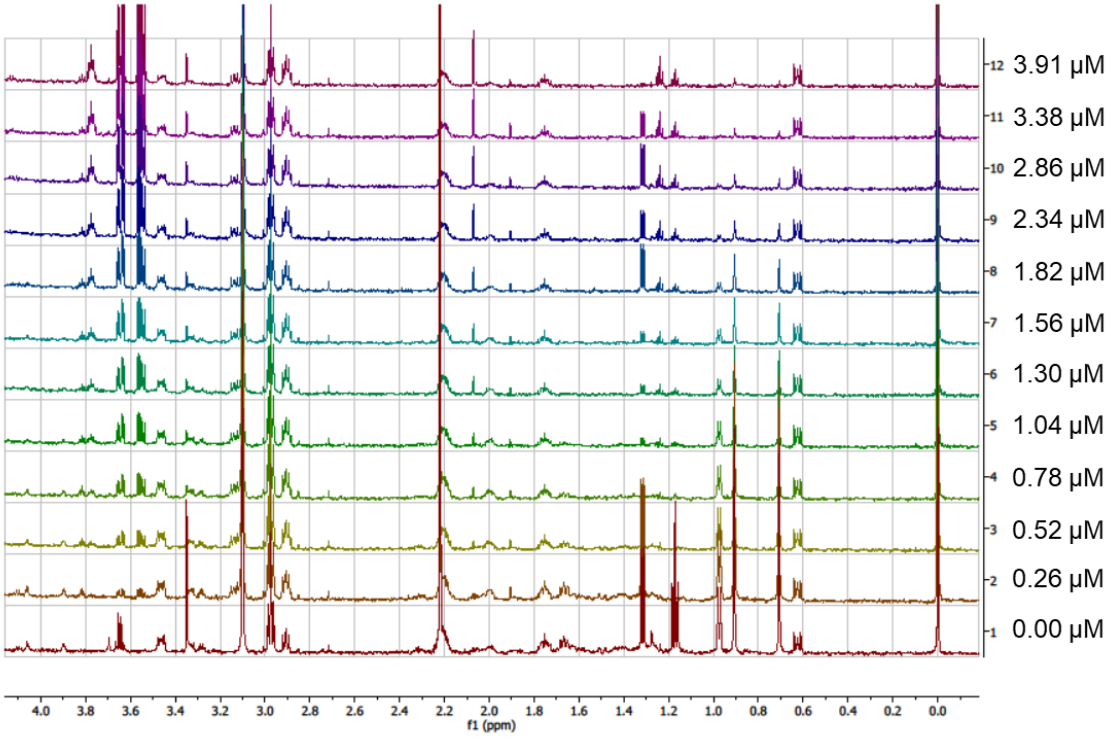

Figure S15 - Raw ^{1}H NMR titration data of **1** against PAO1 nanodiscs, n = 2.

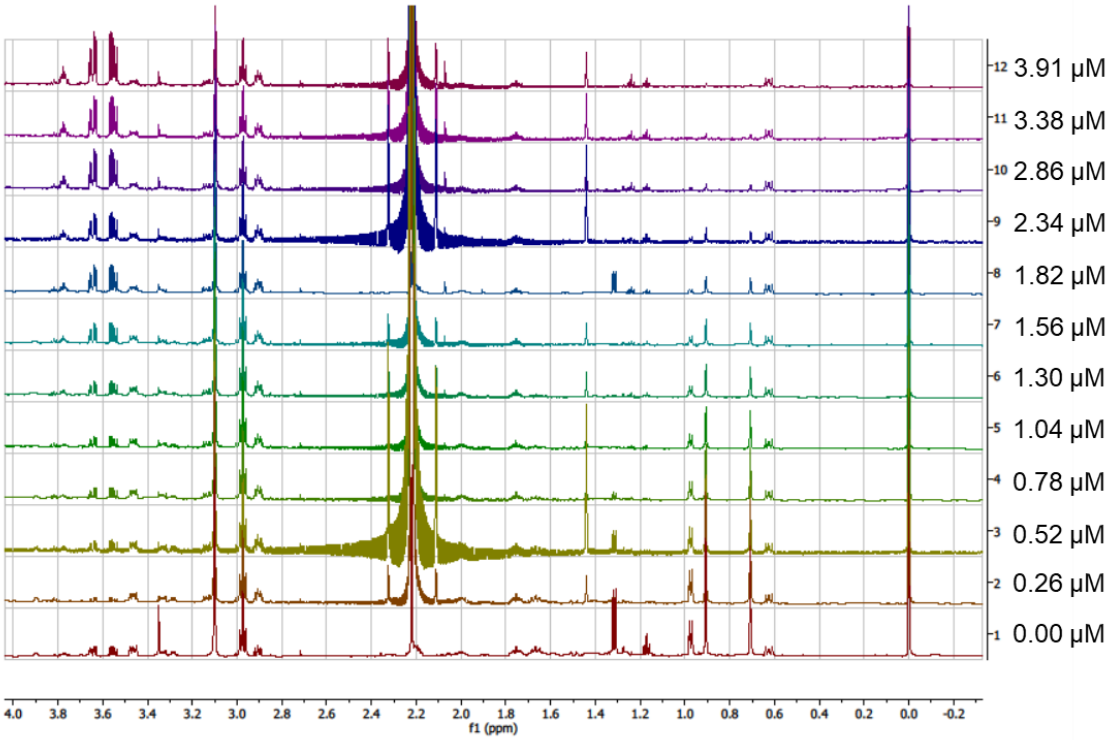

Figure S16 - Raw ^{1}H NMR titration data of **1** against PAO1 nanodiscs, n = 3.

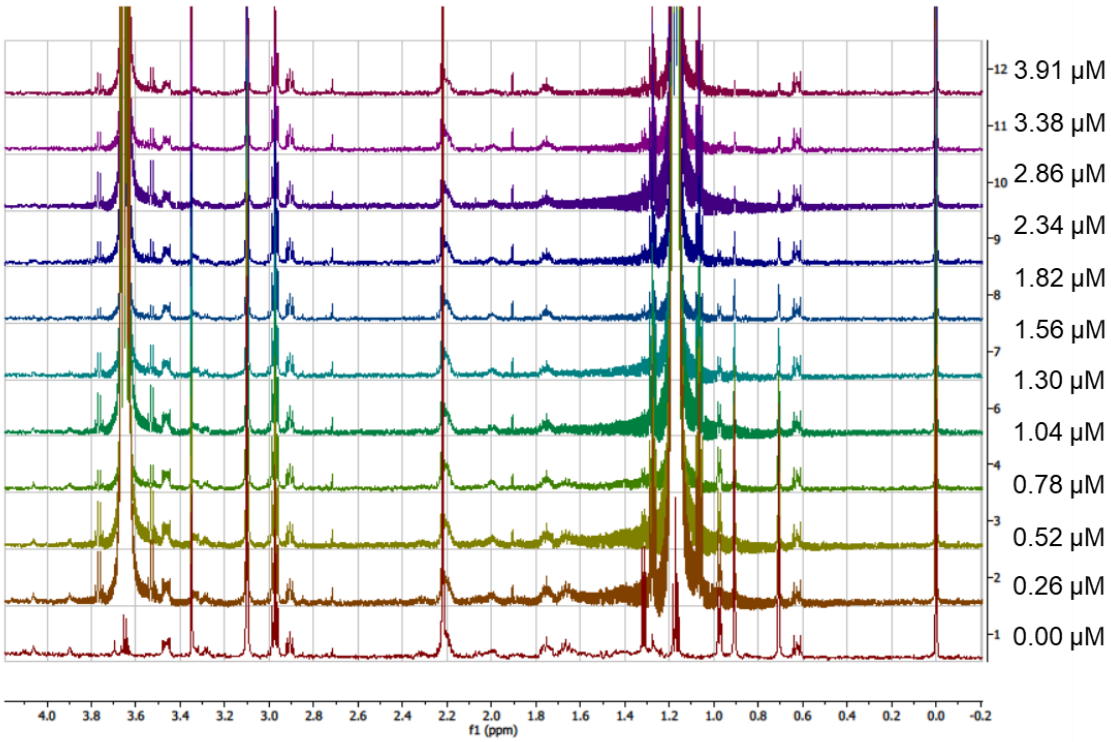

Figure S17 - Raw ^{1}H NMR titration data of **1** against NCTC 13437 nanodiscs, n = 1.

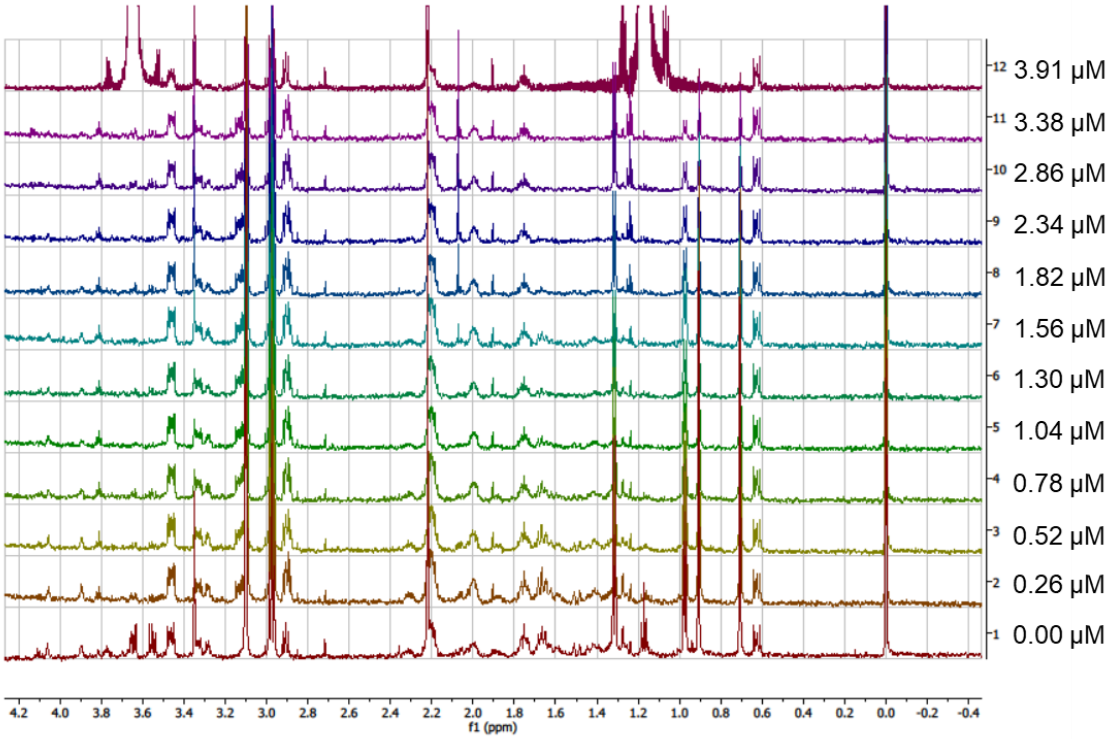

Figure S18 - Raw ^{1}H NMR titration data of **1** against NCTC 13437 nanodiscs, n = 2.

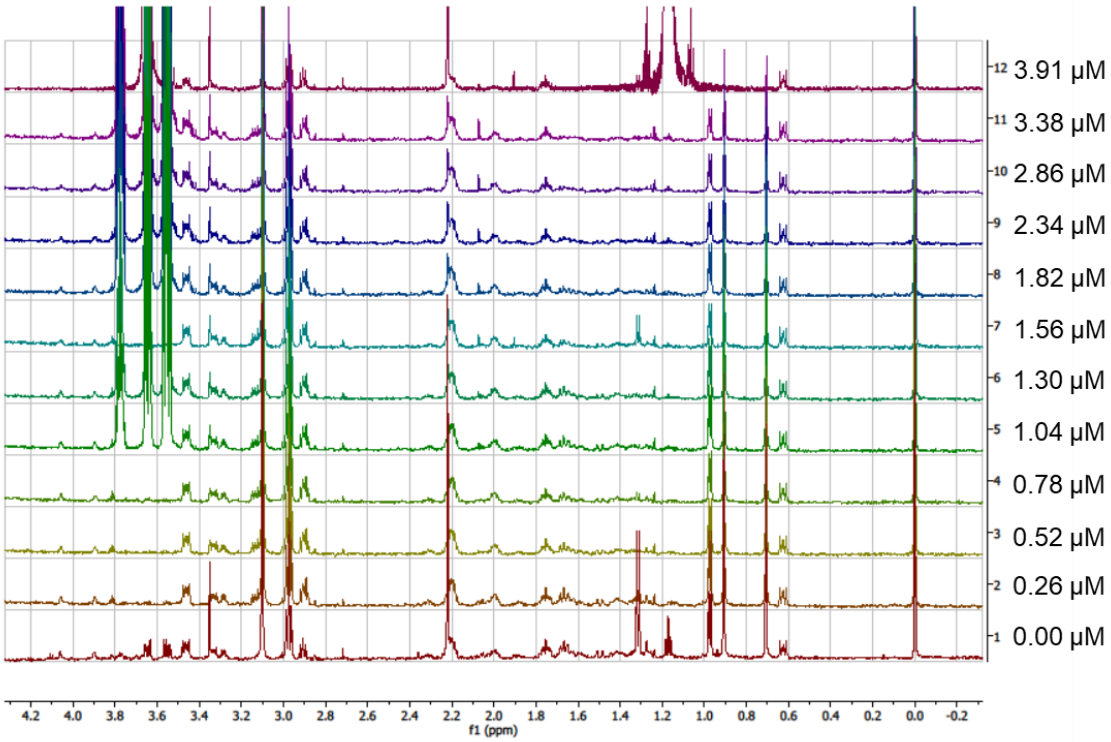

Figure S19 - Raw ^{1}H NMR titration data of **1** against NCTC 13437 nanodiscs, n = 3.

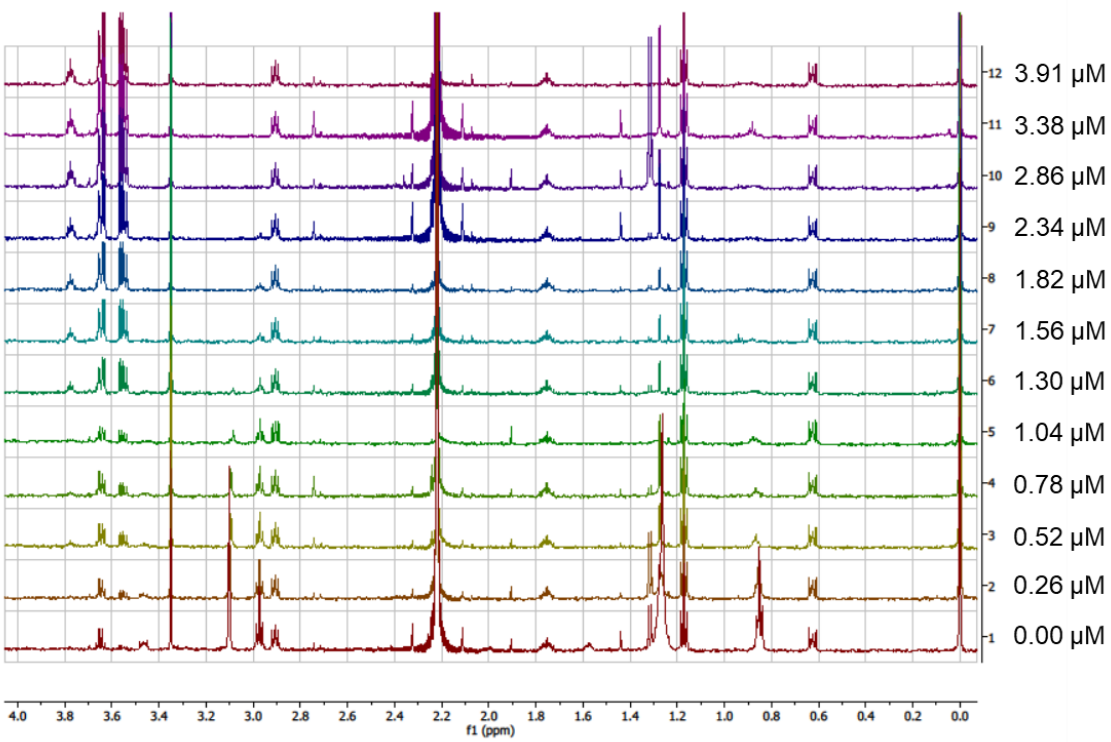

Figure S20 - Raw ^{1}H NMR titration data of **2** against PAO1 nanodiscs.

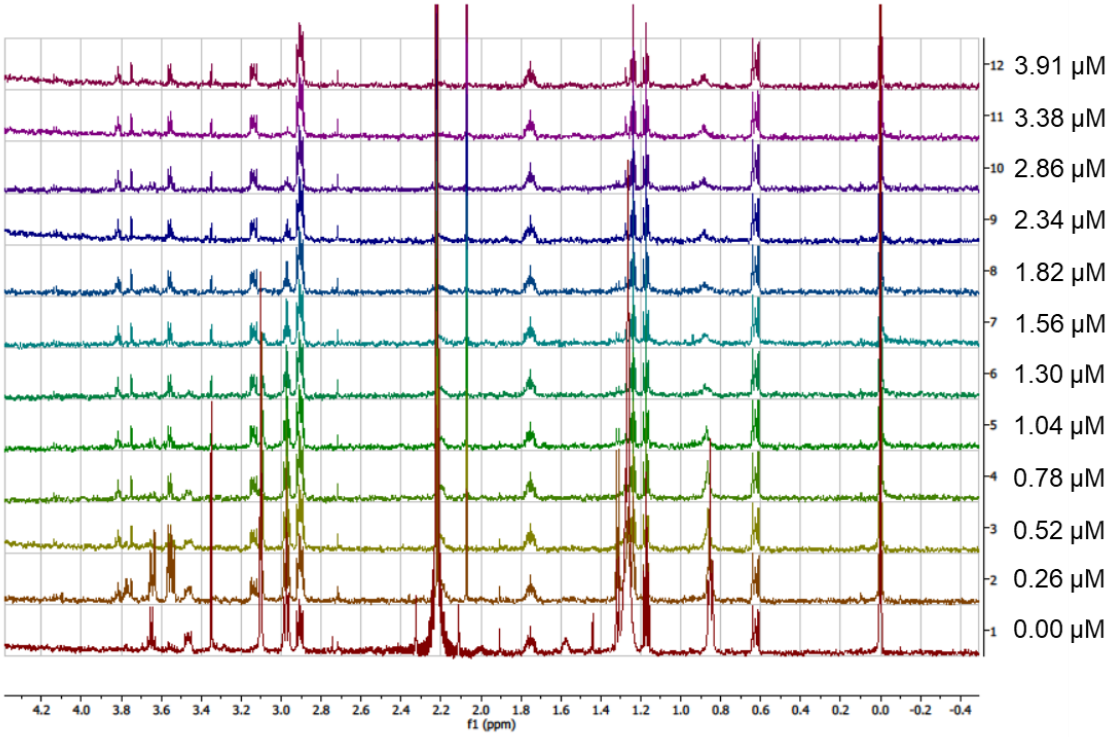

Figure S21 - Raw ^{1}H NMR titration data of **2** against NCTC 13437 nanodiscs.

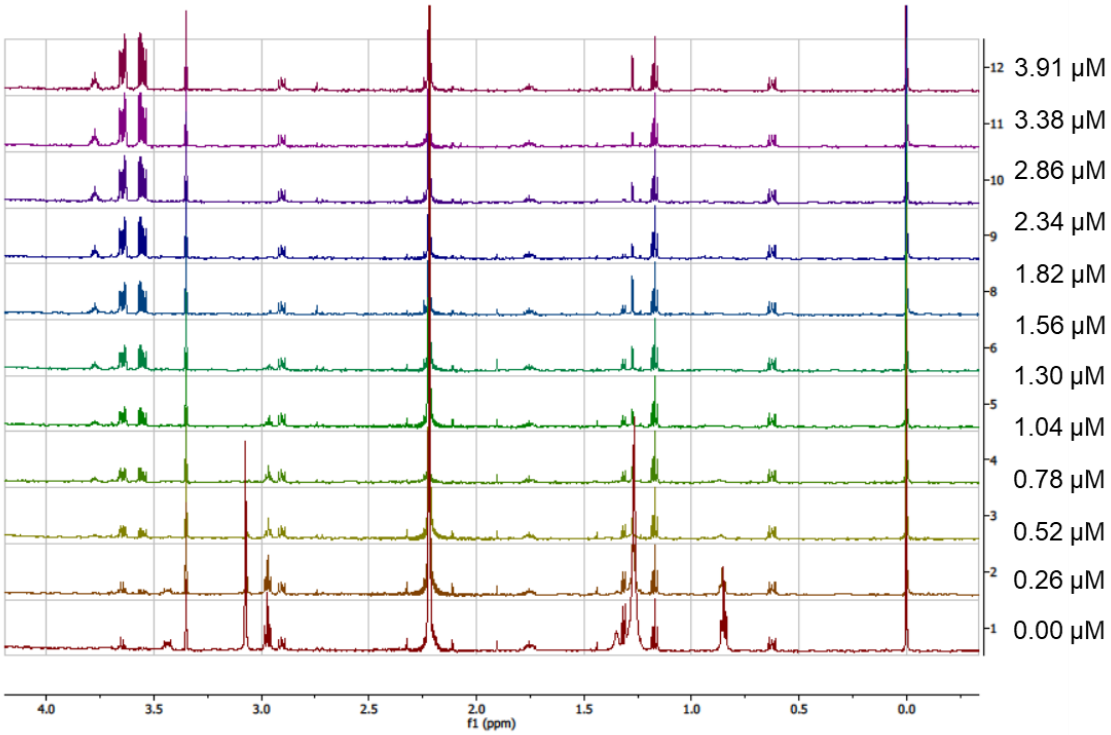

Figure S22 - Raw ^{1}H NMR titration data of **3** against PAO1 nanodiscs.

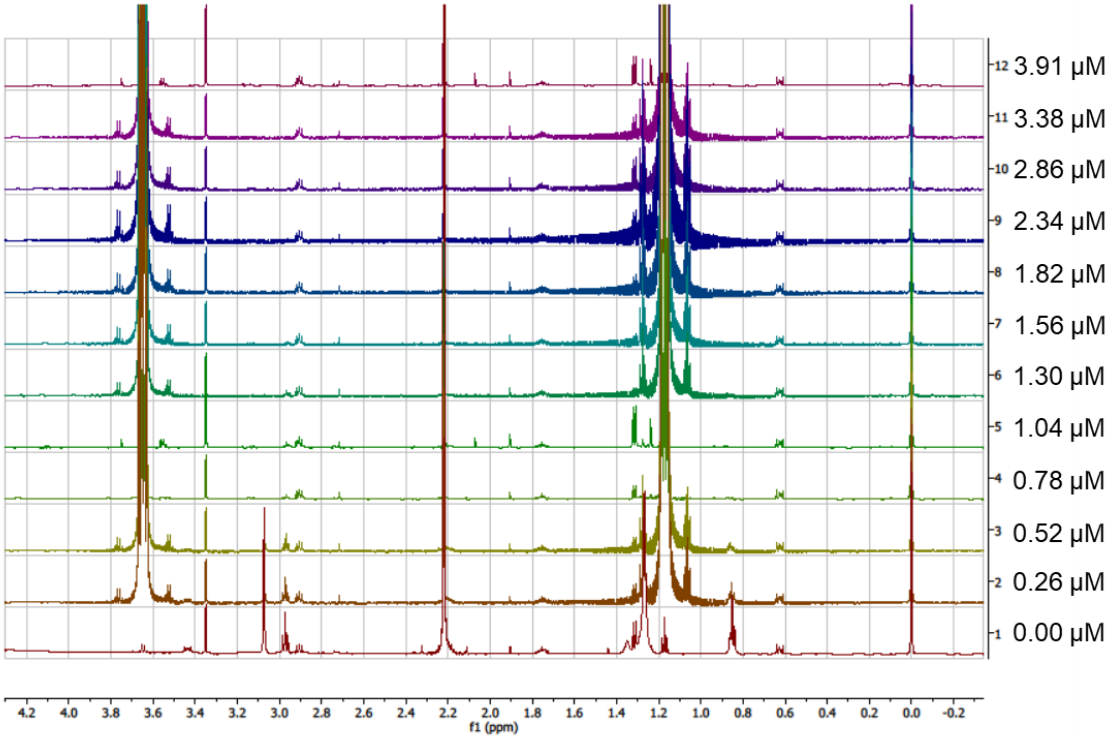

Figure S23 - Raw ^{1}H NMR titration data of **3** against NCTC 13437 nanodiscs.

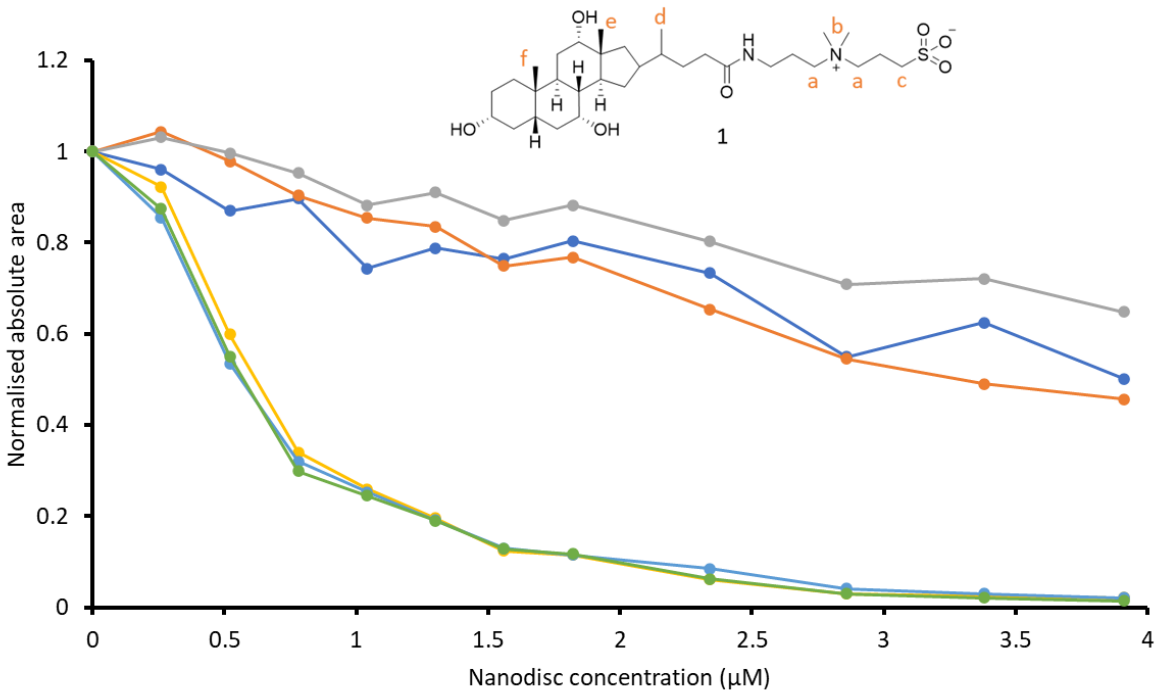

Figure S24 - The relative normalised area of a downfield aromatic resonance of **1** upon titration with PAO1 nanodiscs. Dark blue = a, orange = b, grey = c, yellow = d, light blue = e, green = f.

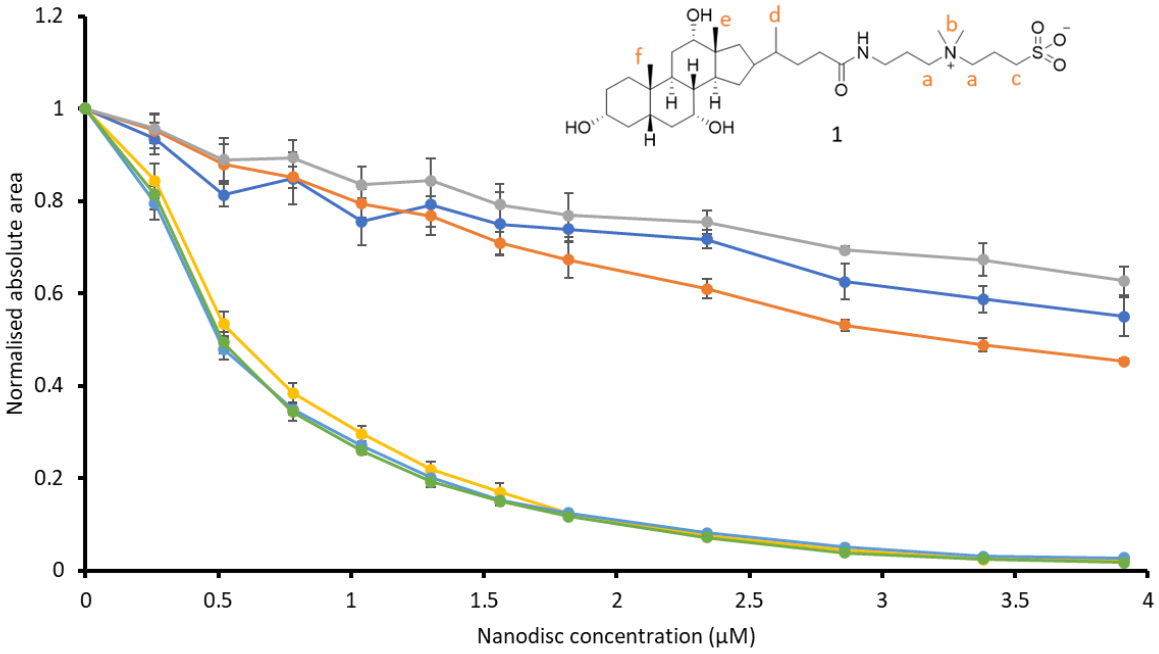

Figure S25 - The relative normalised area of a downfield aromatic resonance of **1** upon titration with PAO1 nanodiscs, n=3, error = standard deviation of the mean. Dark blue = a, orange = b, grey = c, yellow = d, light blue = e, green = f.

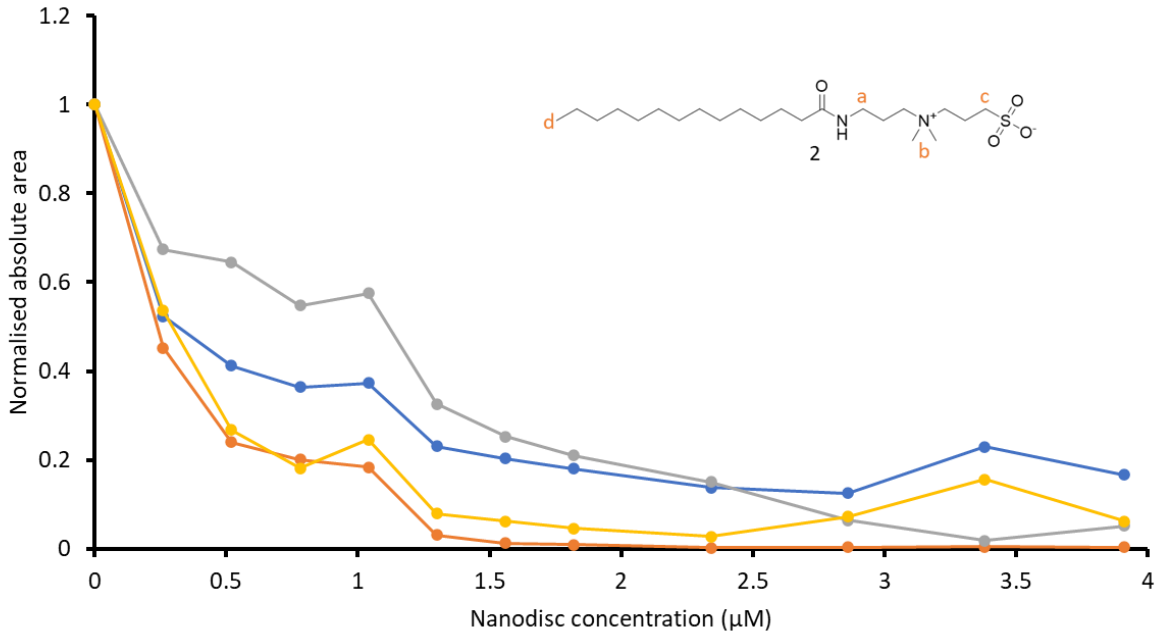

Figure S26 - The relative normalised area of a downfield aromatic resonance of **2** upon titration with PAO1 nanodiscs. Dark blue = a, orange = b, grey = c, yellow = d.

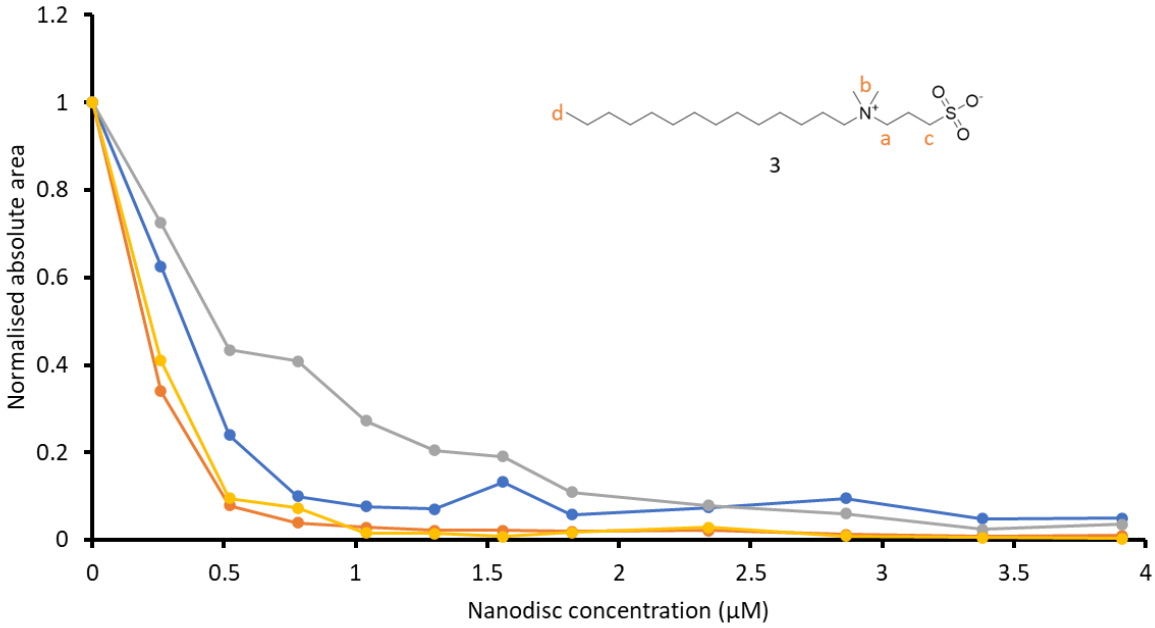

Figure S27 - The relative normalised area of a downfield aromatic resonance of **3** upon titration with PAO1 nanodiscs. Dark blue = a, orange = b, grey = c, yellow = d.

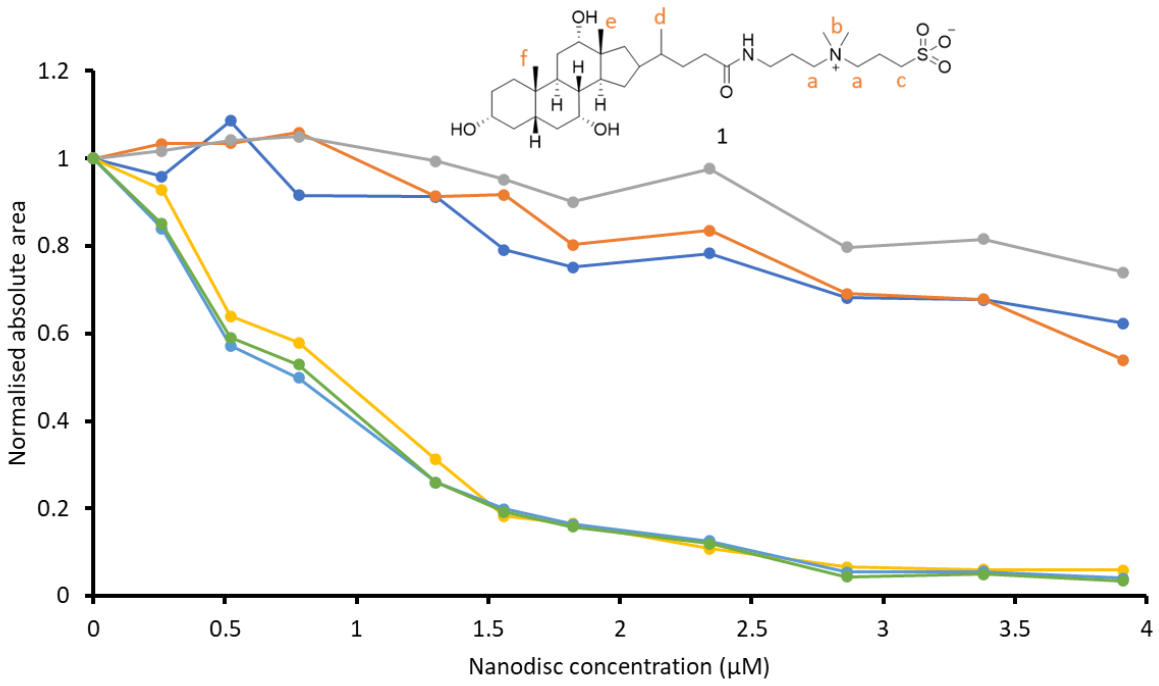

Figure S28 - The relative normalised area of a downfield aromatic resonance of **1** upon titration with NCTC 13437 nanodiscs. Dark blue = a, orange = b, grey = c, yellow = d, light blue = e, green = f.

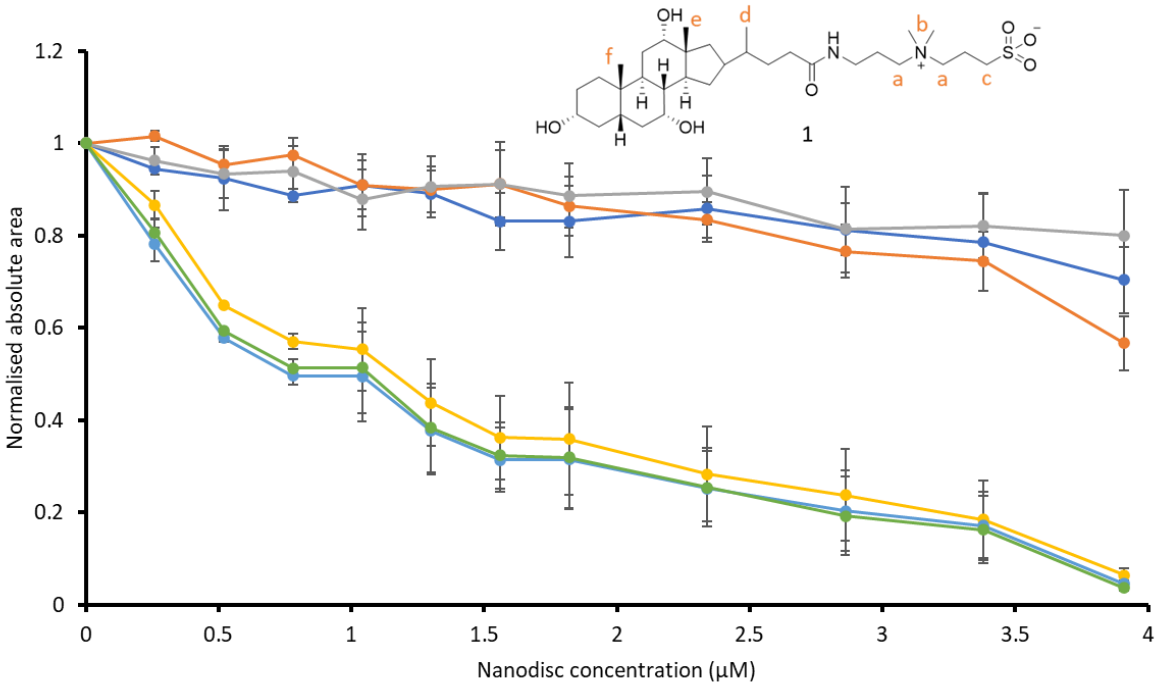

Figure S29 - The relative normalised area of a downfield aromatic resonance of **1** upon titration with NCTC 13437 nanodiscs, n=3, error = standard error of the mean. Dark blue = a, orange = b, grey = c, yellow = d, light blue = e, green = f.

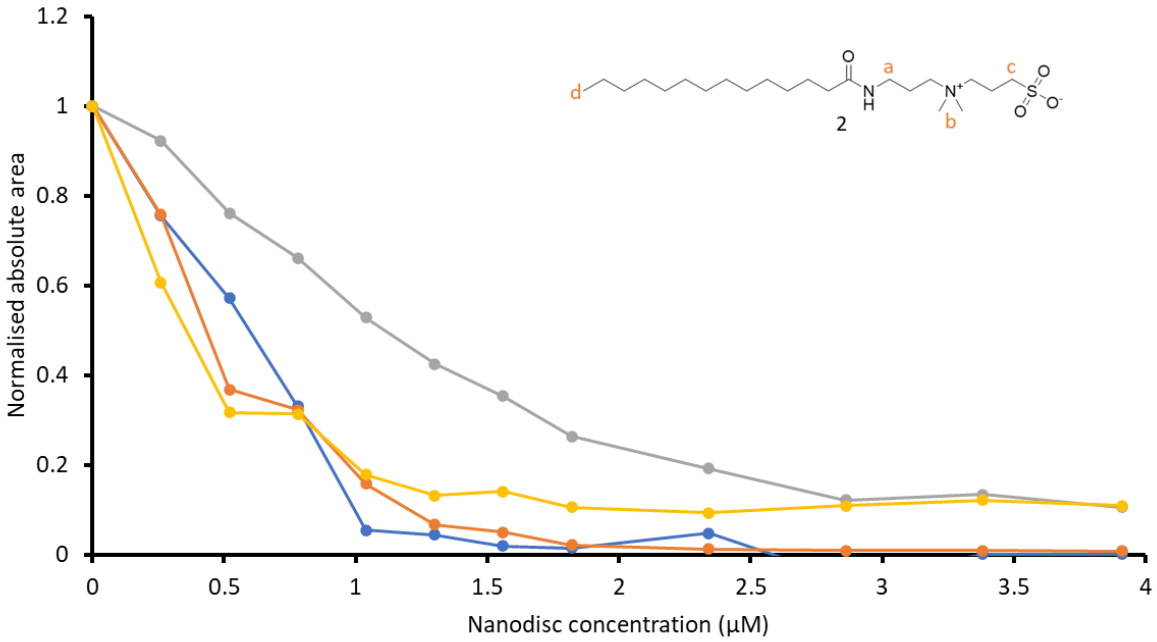

Figure S30 - The relative normalised area of a downfield aromatic resonance of **2** upon titration with NCTC 13437 nanodiscs. Dark blue = a, orange = b, grey = c, yellow = d.

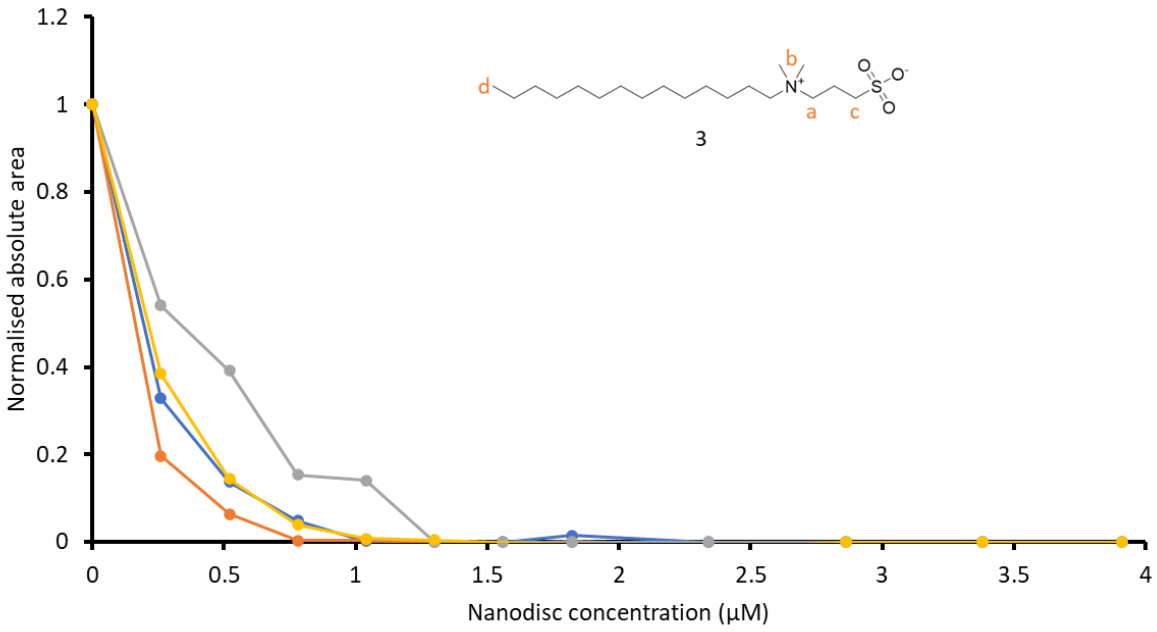

Figure S31 - The relative normalised area of a downfield aromatic resonance of **3** upon titration with NCTC 13437 nanodiscs. Dark blue = a, orange = b, grey = c, yellow = d.

Section 9: EC_{50} determination

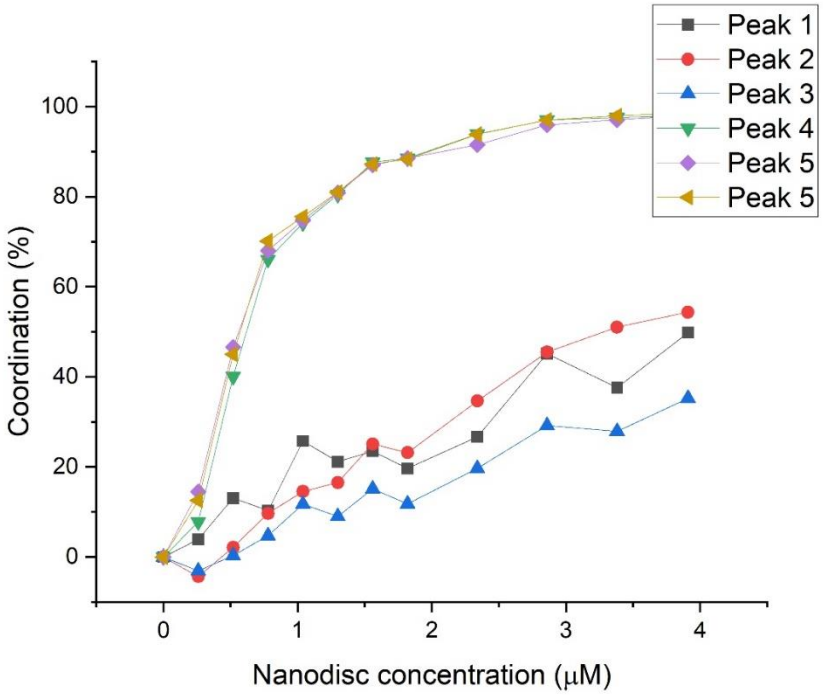

Figure S32 - Graph showing the percentage of **1** coordinated to PAO1 nanodiscs, with respect to increasing nanodisc concentration.

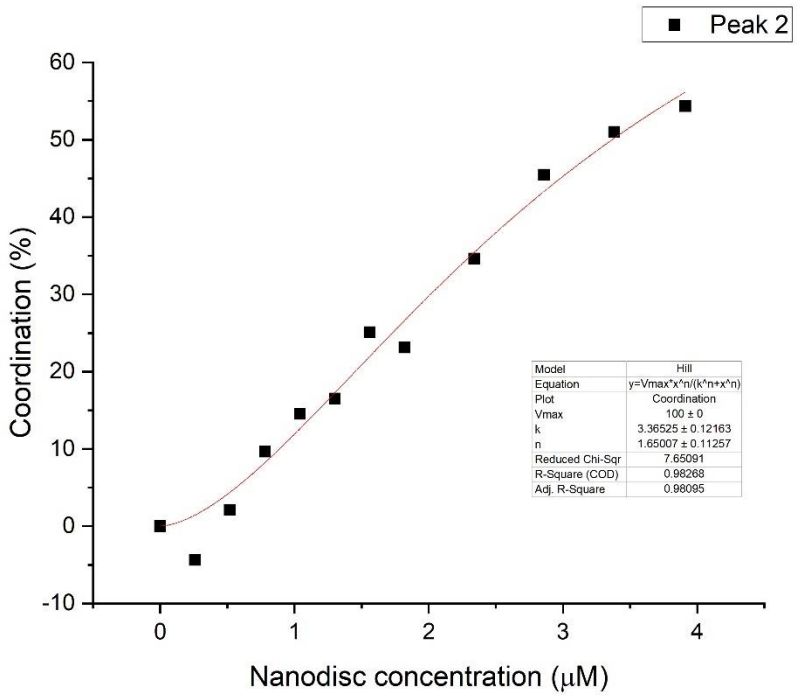

Figure S33 - Graph showing the percentage of **1**, peak 2 coordinated to PAO1 nanodiscs, with respect to increasing nanodisc concentration. Data was then fitted to the Hill Plot model with V_{max} fixed at 100 %.

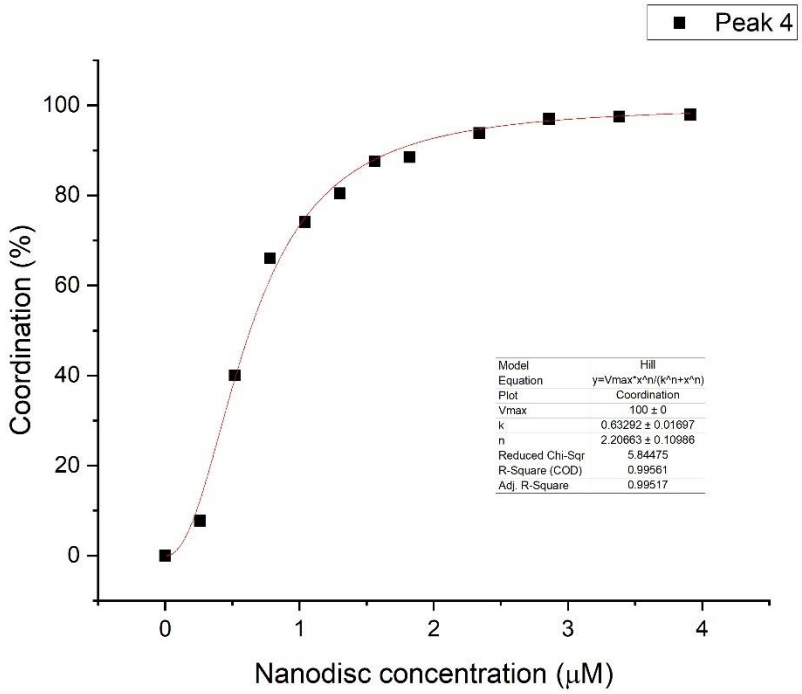

Figure S34 - Graph showing the percentage of **1**, peak d/4 coordinated to PAO1 nanodiscs, with respect to increasing nanodisc concentration. Data was then fitted to the Hill Plot model with V_{max} fixed at 100 %.

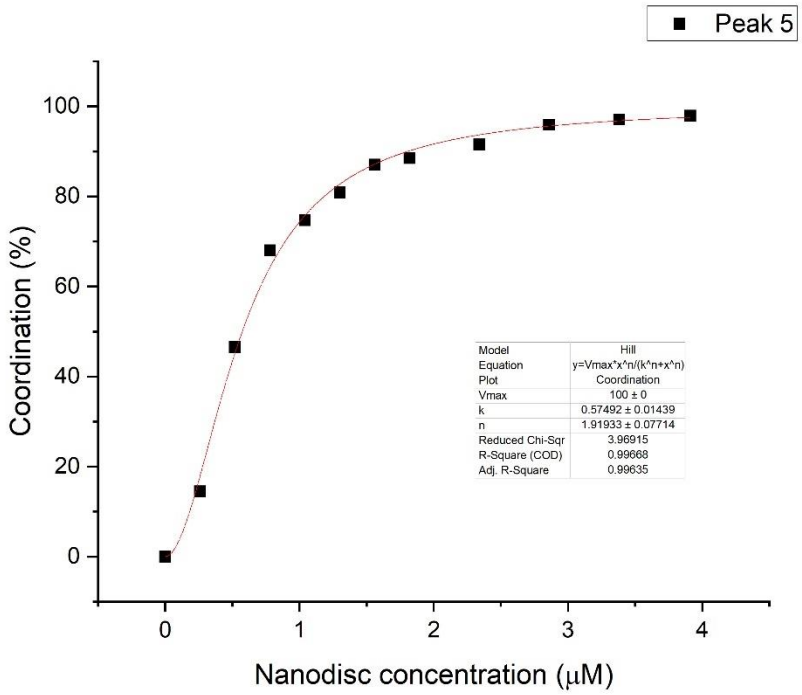

Figure S35 - Graph showing the percentage of **1**, peak e/5 coordinated to PAO1 nanodiscs, with respect to increasing nanodisc concentration. Data was then fitted to the Hill Plot model with V_{max} fixed at 100 %.

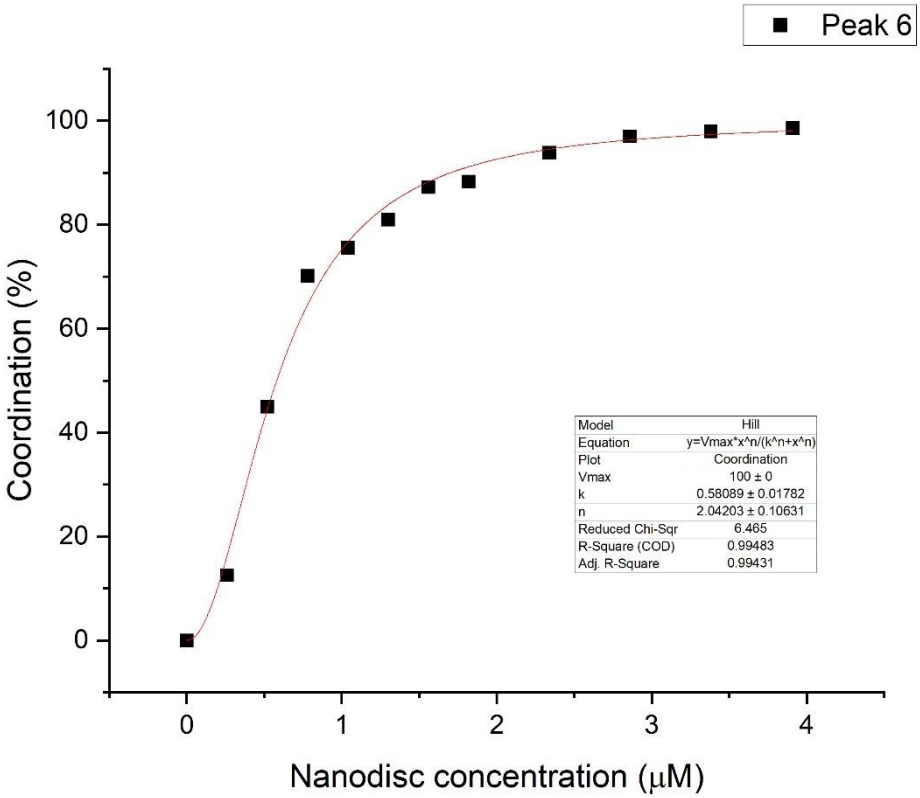

Figure S36 - Graph showing the percentage of **1**, peak f/6 coordinated to PAO1 nanodiscs, with respect to increasing nanodisc concentration. Data was then fitted to the Hill Plot model with V_{max} fixed at 100 %.

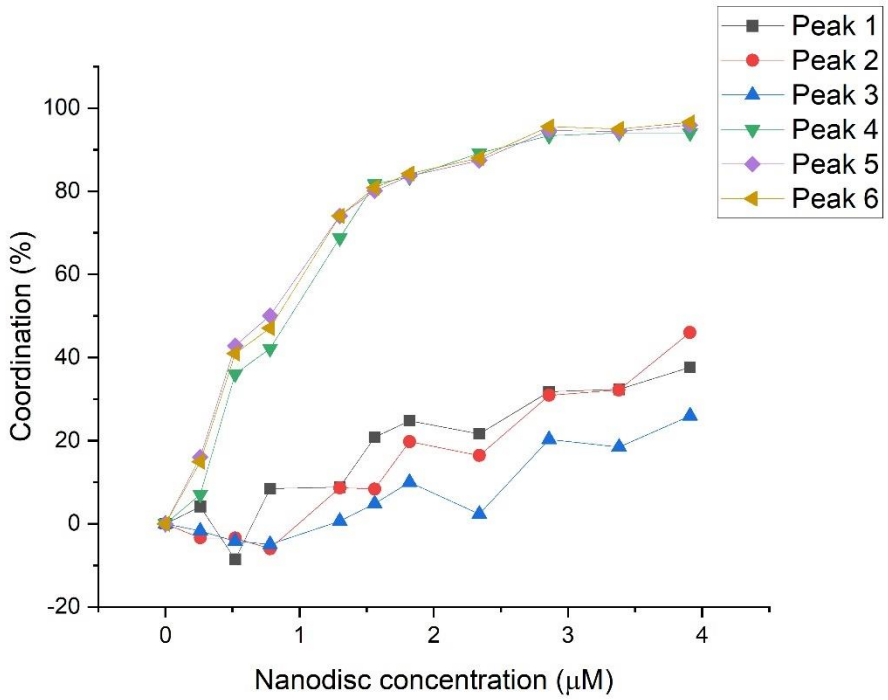

Figure S37 - Graph showing the percentage of **1** coordinated to NCTC 13437 nanodiscs, with respect to increasing nanodisc concentration.

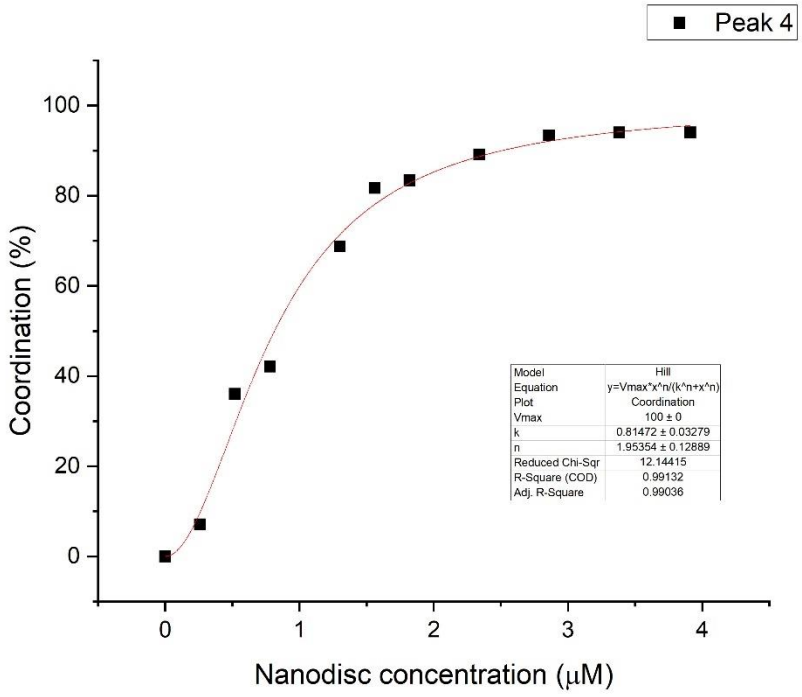

Figure S38 - Graph showing the percentage of **1**, peak d/4 coordinated to NCTC 13437 nanodiscs, with respect to increasing nanodisc concentration. Data was then fitted to the Hill Plot model with V_{max} fixed at 100 %.

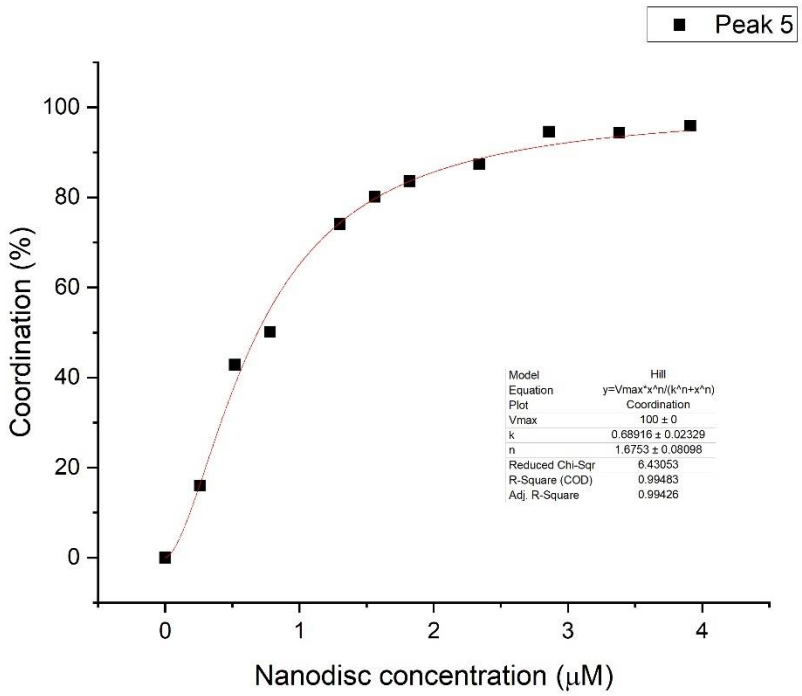

Figure S39 - Graph showing the percentage of **1**, peak e/5 coordinated to NCTC 13437 nanodiscs, with respect to increasing nanodisc concentration. Data was then fitted to the Hill Plot model with V_{max} fixed at 100 %.

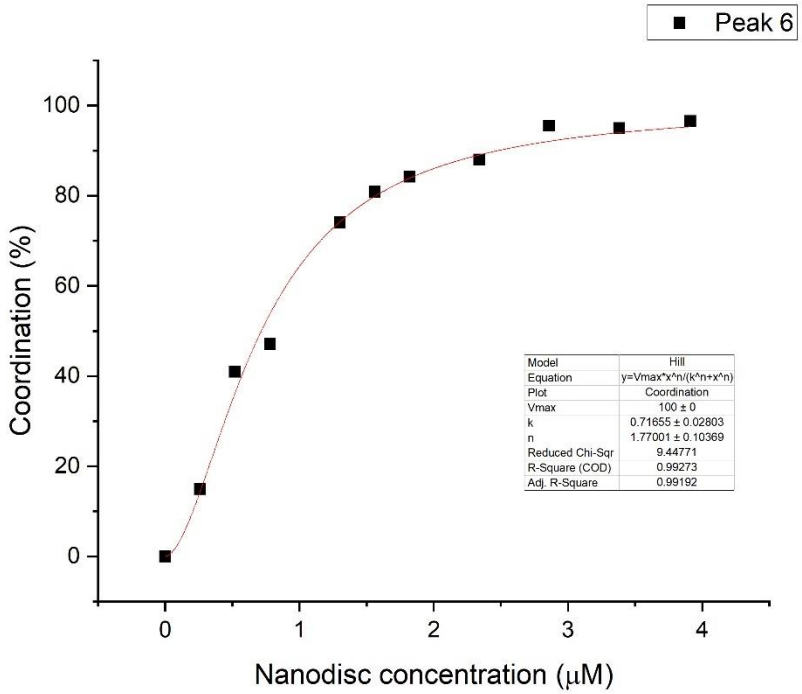

Figure S40 - Graph showing the percentage of **1**, peak f/6 coordinated to NCTC 13437 nanodiscs, with respect to increasing nanodisc concentration. Data was then fitted to the Hill Plot model with V_{max} fixed at 100 %.

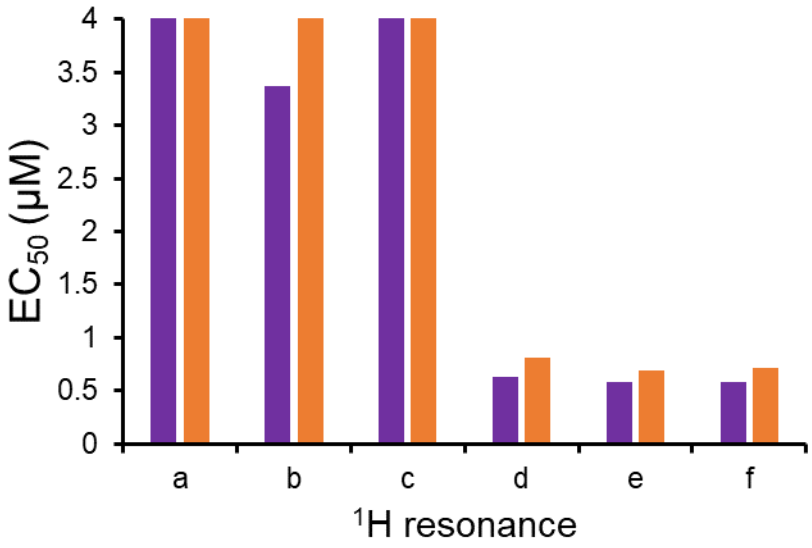

Figure S41 - EC_{50} (μM) values obtained from the fitting of peaks a – f of **1** titration data to Hill Plot kinetics using Origin 2018 software, with V_{max} fixed to 100 % of **1** bound to the nanodisc. Purple = results from PAO1 nanodiscs, orange = results from NCTC 13437 nanodiscs.

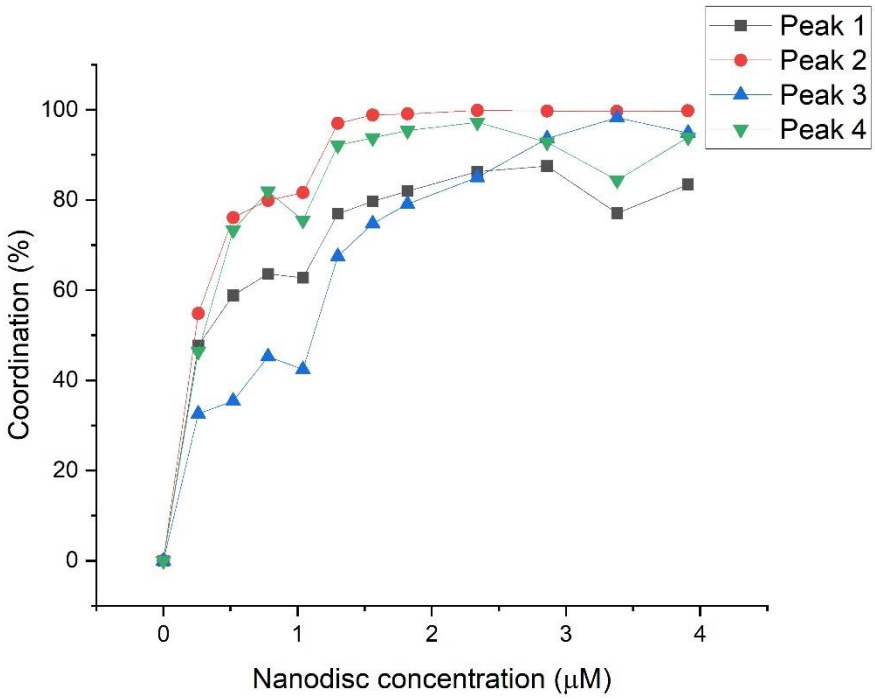

Figure S42 - Graph showing the percentage of **2** coordinated to PAO1 nanodiscs, with respect to increasing nanodisc concentration.

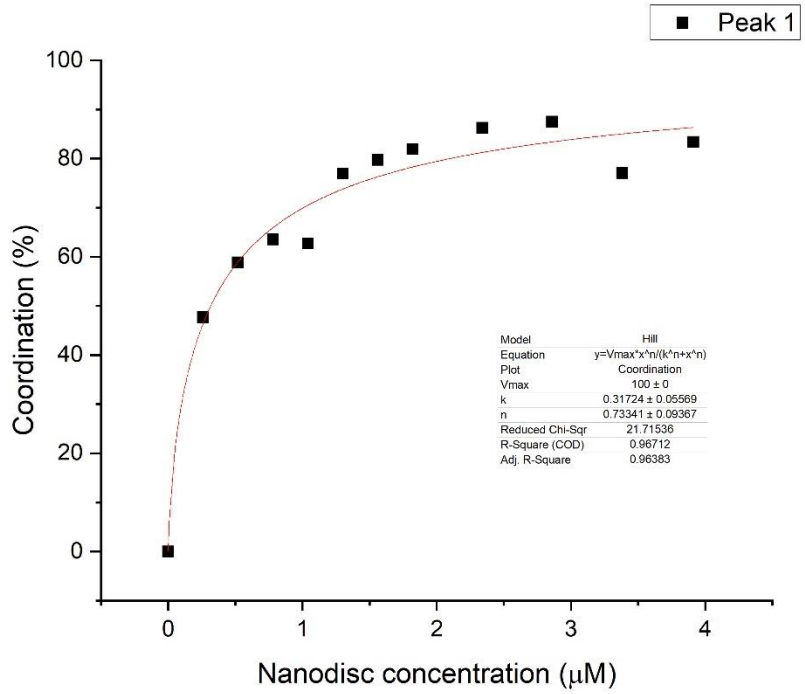

e

Figure S43 - Graph showing the percentage of **2**, peak a/1 coordinated to PAO1 nanodiscs, with respect to increasing nanodisc concentration. Data was then fitted to the Hill Plot model with V_{max} fixed at 100 %.

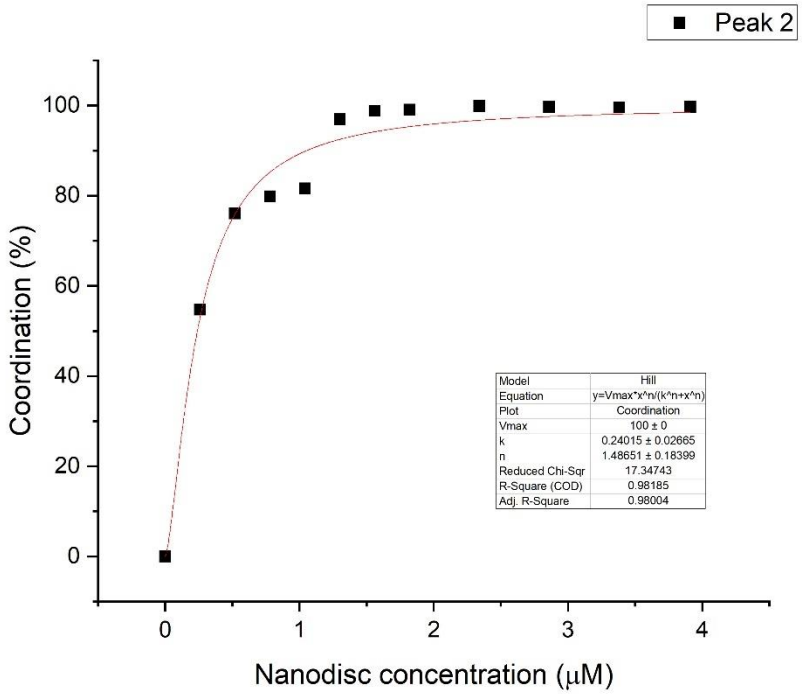

Figure S44 - Graph showing the percentage of **2**, peak b/2 coordinated to PAO1 nanodiscs, with respect to increasing nanodisc concentration. Data was then fitted to the Hill Plot model with V_{max} fixed at 100 %.

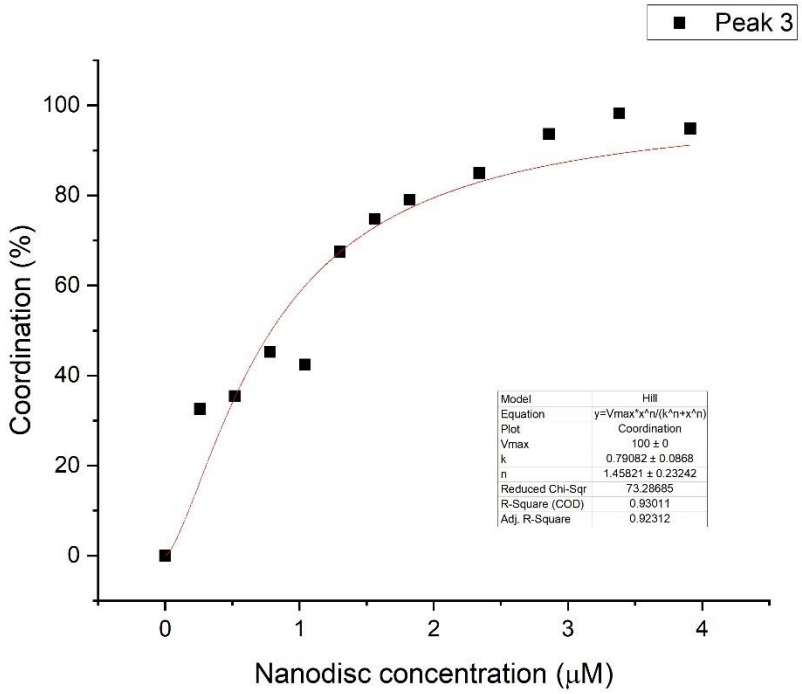

Figure S45 - Graph showing the percentage of **2**, peak c/3 coordinated to PAO1 nanodiscs, with respect to increasing nanodisc concentration. Data was then fitted to the Hill Plot model with V_{max} fixed at 100 %.

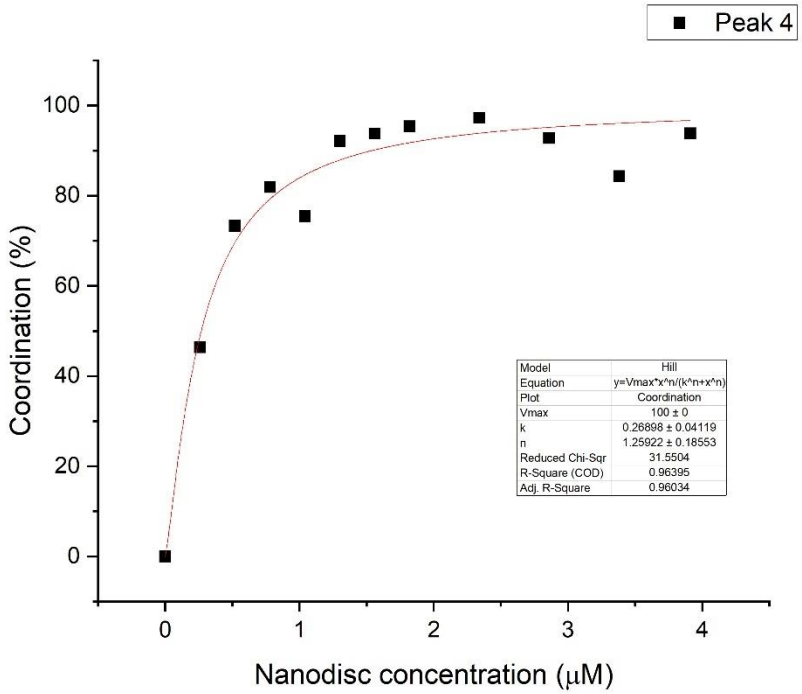

Figure S46 - Graph showing the percentage of **2**, peak d/4 coordinated to PAO1 nanodiscs, with respect to increasing nanodisc concentration. Data was then fitted to the Hill Plot model with V_{max} fixed at 100 %.

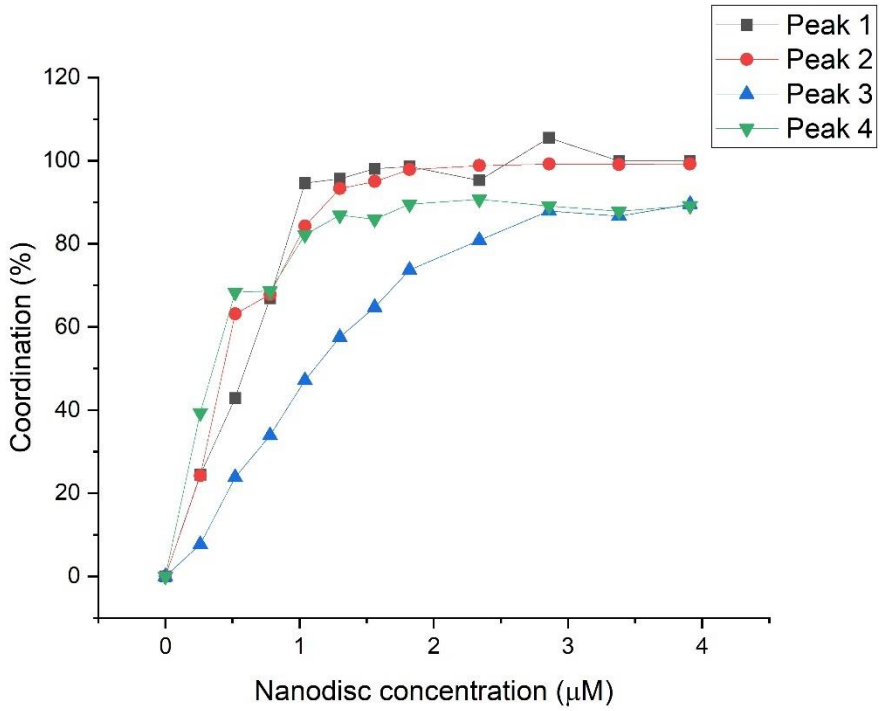

Figure S47 - Graph showing the percentage of **2** coordinated to NCTC 13437 nanodiscs, with respect to increasing nanodisc concentration.

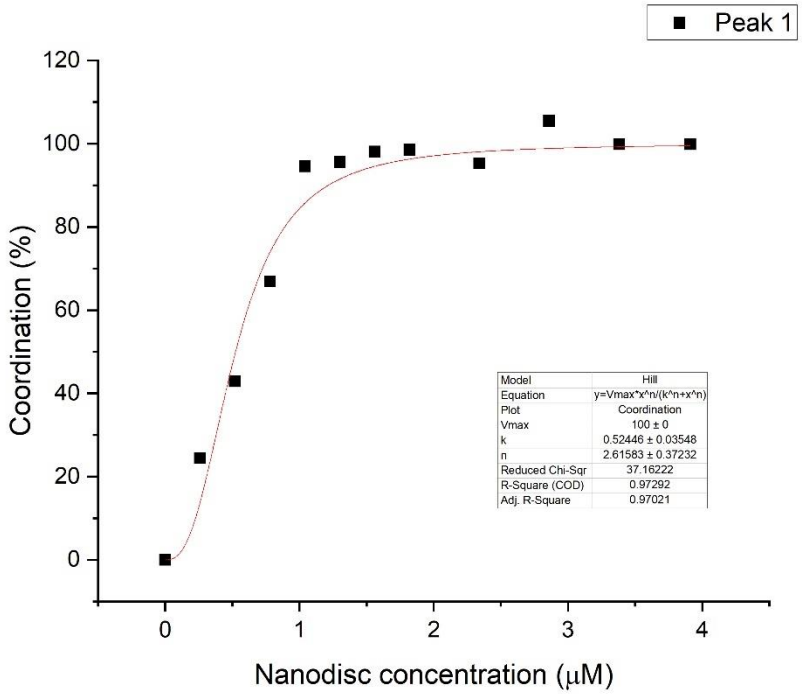

Figure S48 - Graph showing the percentage of **2**, peak a/1 coordinated to NCTC 13437 nanodiscs, with respect to increasing nanodisc concentration. Data was then fitted to the Hill Plot model with V_{max} fixed at 100 %.

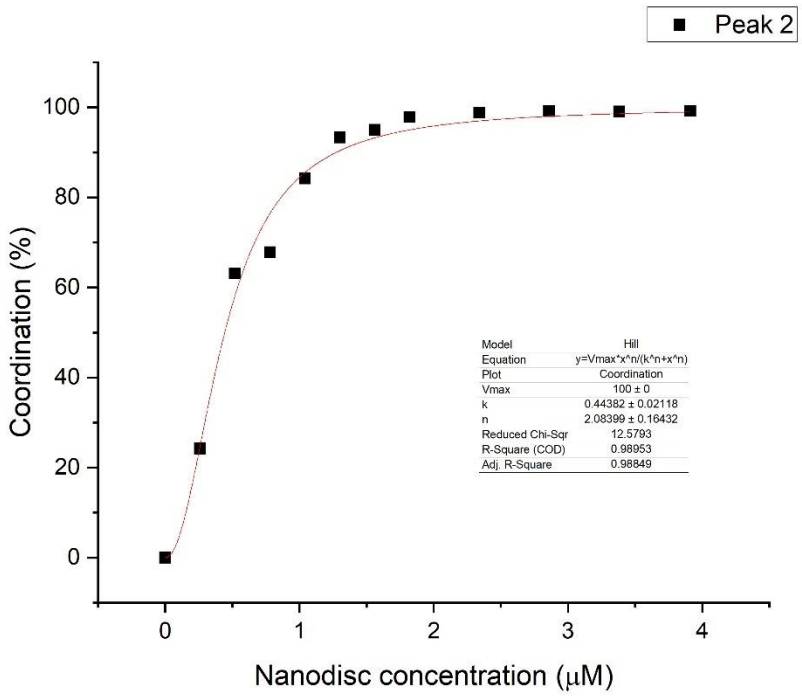

Figure S49 - Graph showing the percentage of **2**, peak b/2 coordinated to NCTC 13437 nanodiscs, with respect to increasing nanodisc concentration. Data was then fitted to the Hill Plot model with V_{max} fixed at 100 %.

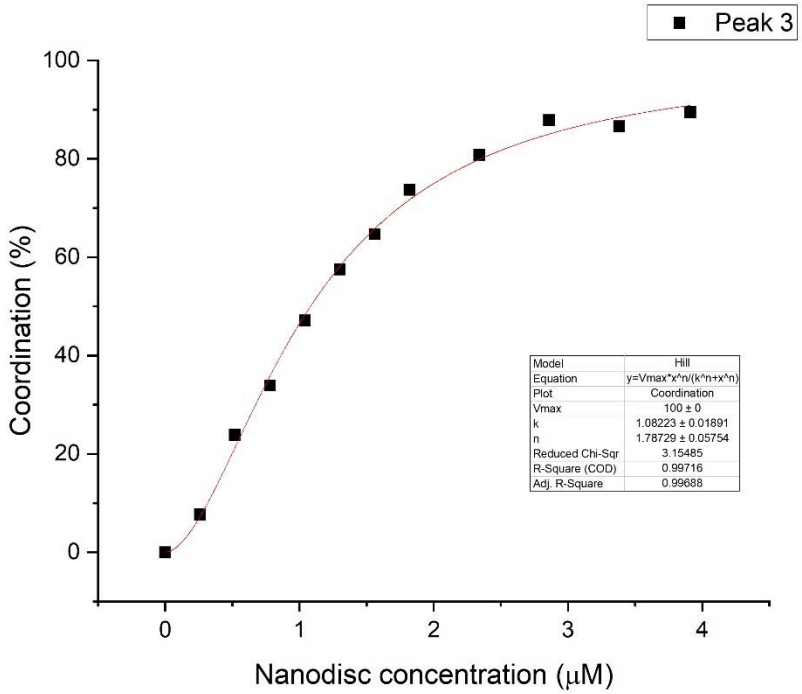

Figure S50 - Graph showing the percentage of **2**, peak c/3 coordinated to NCTC 13437 nanodiscs, with respect to increasing nanodisc concentration. Data was then fitted to the Hill Plot model with V_{max} fixed at 100 %.

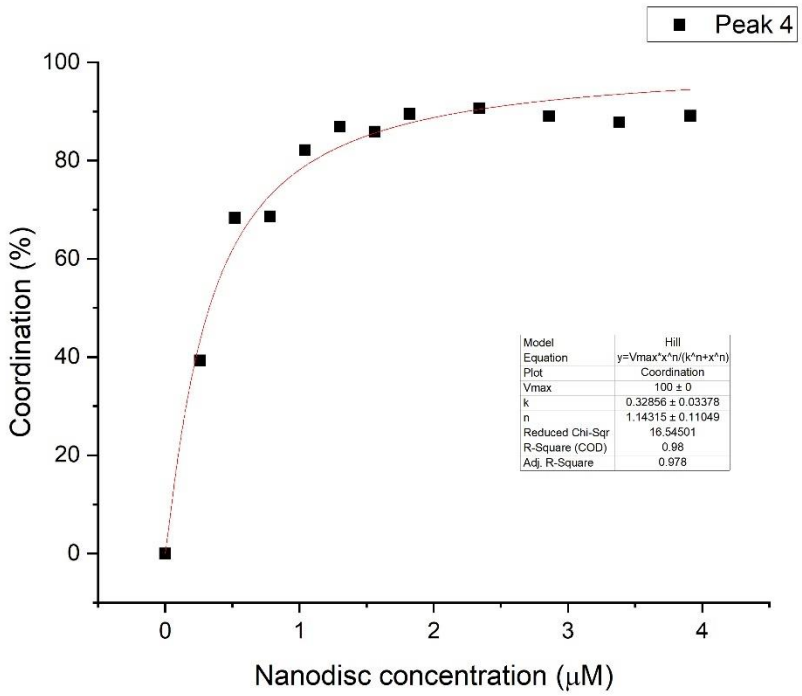

Figure S51 - Graph showing the percentage of **2**, peak d/4 coordinated to NCTC 13437 nanodiscs, with respect to increasing nanodisc concentration. Data was then fitted to the Hill Plot model with V_{max} fixed at 100 %.

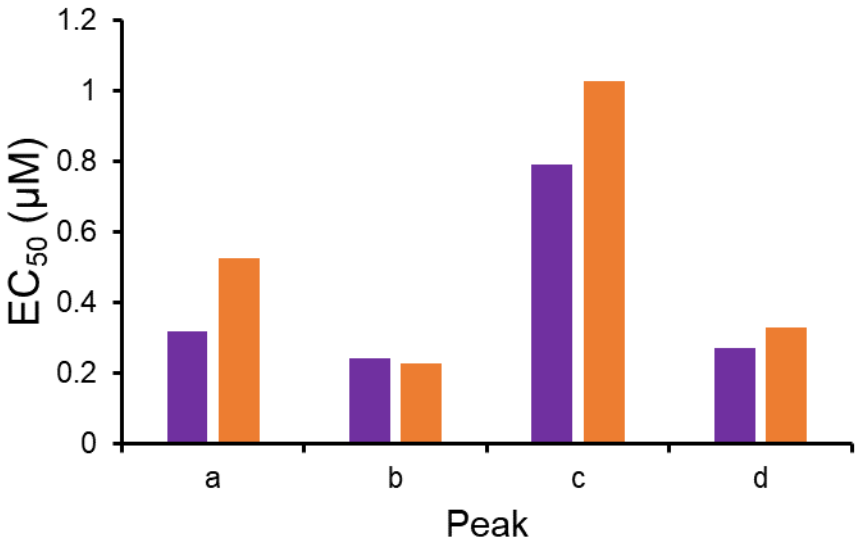

Figure S52 - EC_{50} (μM) values obtained from the fitting of peaks a - d of **2** titration data to Hill Plot kinetics using Origin 2018 software, with V_{max} fixed to 100 % of **2** bound to the nanodisc. Purple = results from PAO1 nanodiscs, orange = results from NCTC 13437 nanodiscs.

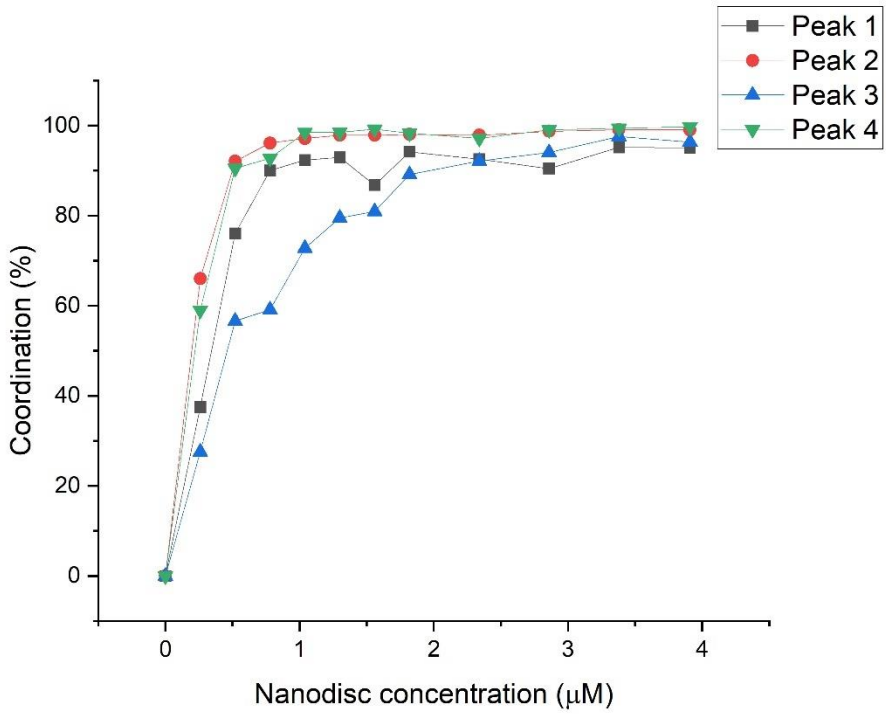

Figure S53 - Graph showing the percentage of **3** coordinated to PAO1 nanodiscs, with respect to increasing nanodisc concentration.

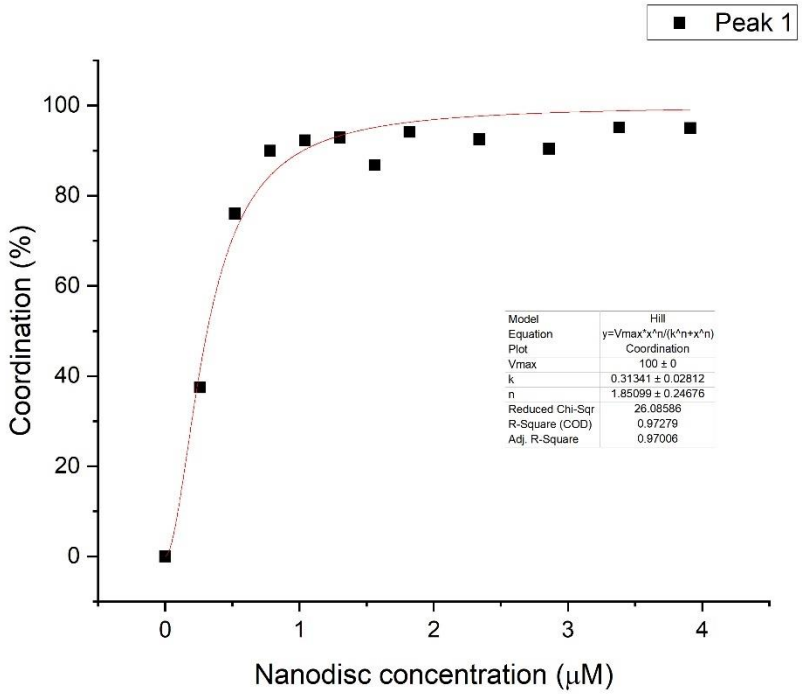

Figure S54 - Graph showing the percentage of **3**, peak a/1 coordinated to PAO1 nanodiscs, with respect to increasing nanodisc concentration. Data was then fitted to the Hill Plot model with V_{max} fixed at 100 %.

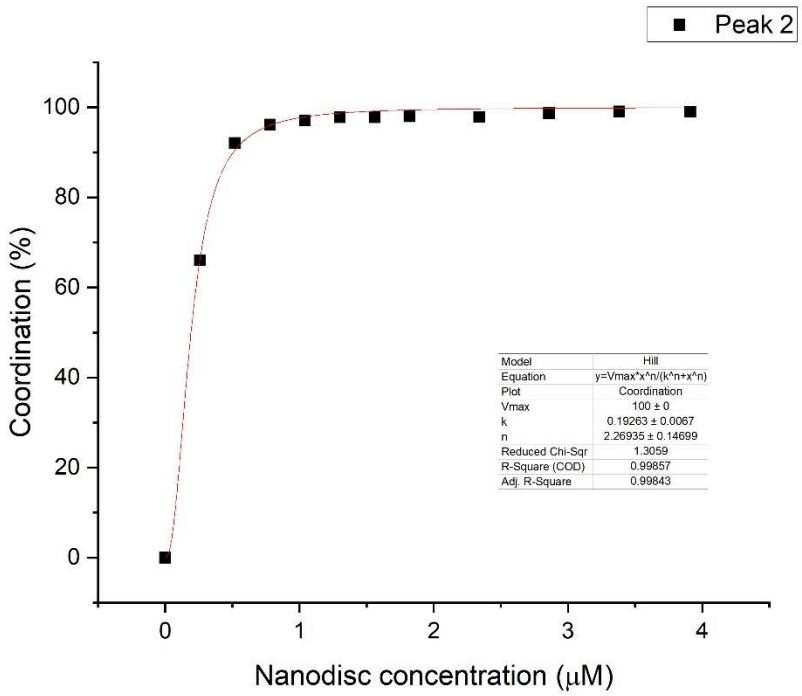

Figure S55 - Graph showing the percentage of **3**, peak b/2 coordinated to PAO1 nanodiscs, with respect to increasing nanodisc concentration. Data was then fitted to the Hill Plot model with V_{max} fixed at 100 %.

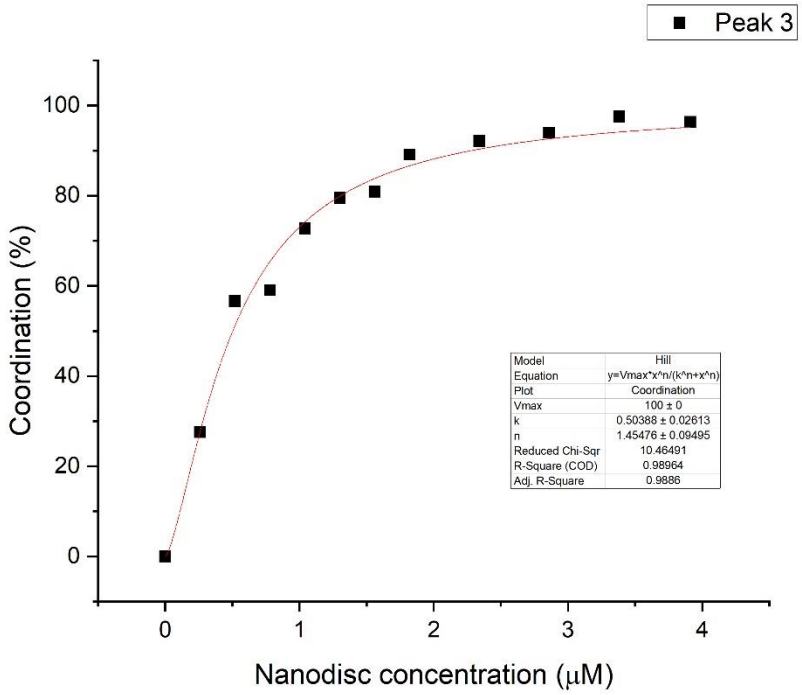

Figure S56 - Graph showing the percentage of **3**, peak c/3 coordinated to PAO1 nanodiscs, with respect to increasing nanodisc concentration. Data was then fitted to the Hill Plot model with V_{max} fixed at 100 %.

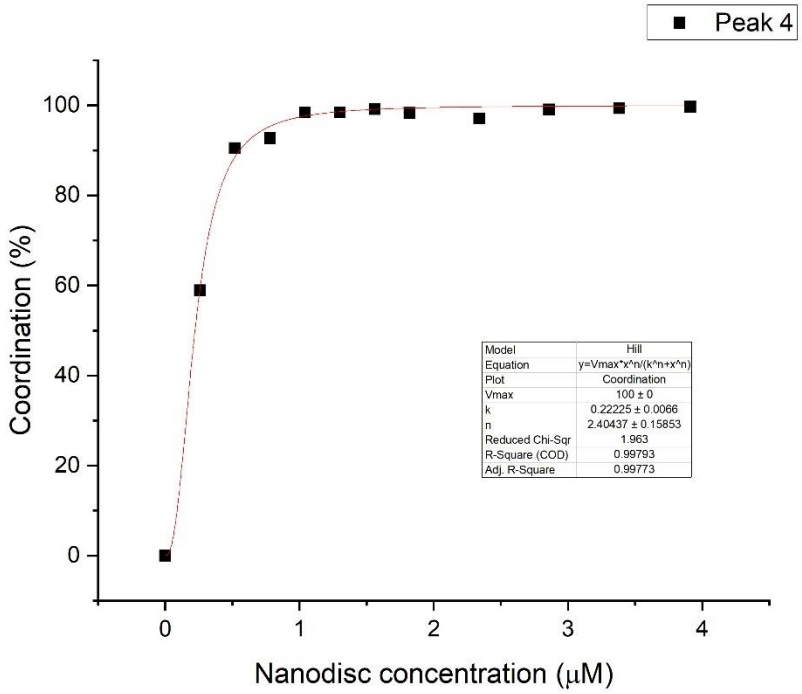

Figure S57 - Graph showing the percentage of **3**, peak d/4 coordinated to PAO1 nanodiscs, with respect to increasing nanodisc concentration. Data was then fitted to the Hill Plot model with V_{max} fixed at 100 %.

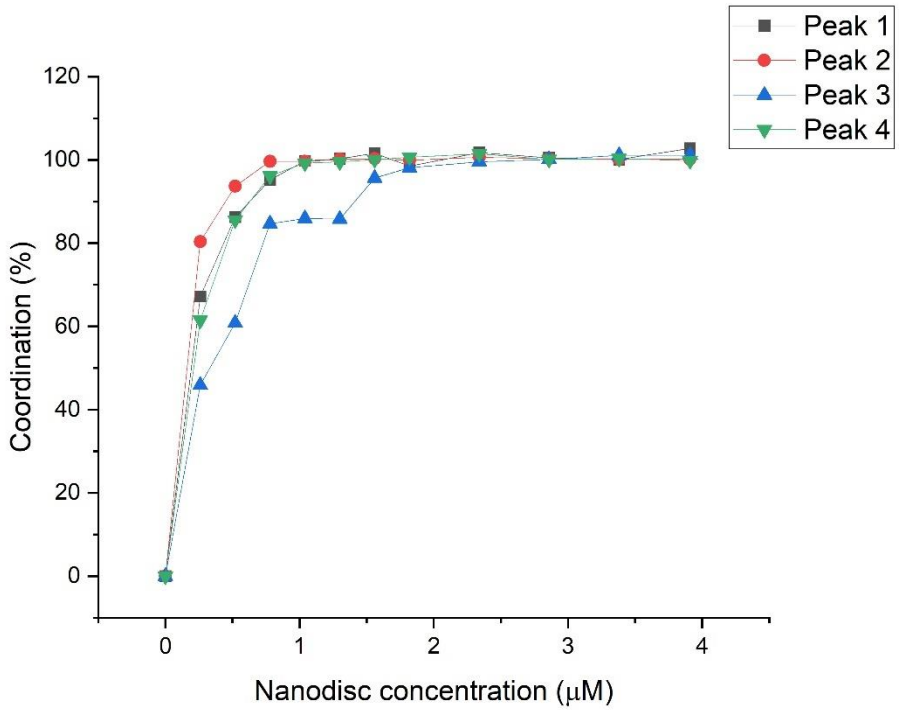

Figure S58 - Graph showing the percentage of **3** coordinated to NCTC 13437 nanodiscs, with respect to increasing nanodisc concentration.

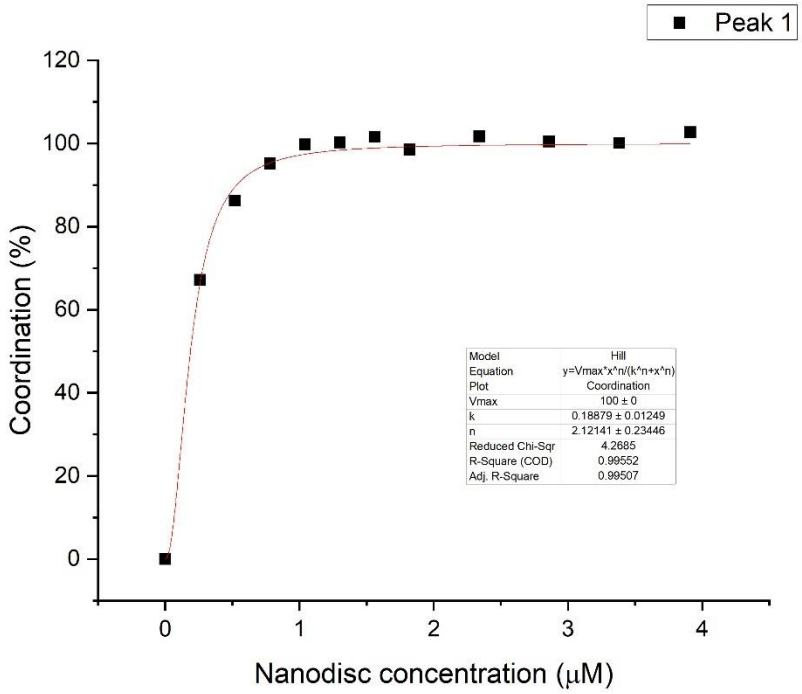

Figure S59 - Graph showing the percentage of **3**, peak a/1 coordinated to NCTC 13437 nanodiscs, with respect to increasing nanodisc concentration. Data was then fitted to the Hill Plot model with V_{max} fixed at 100 %.

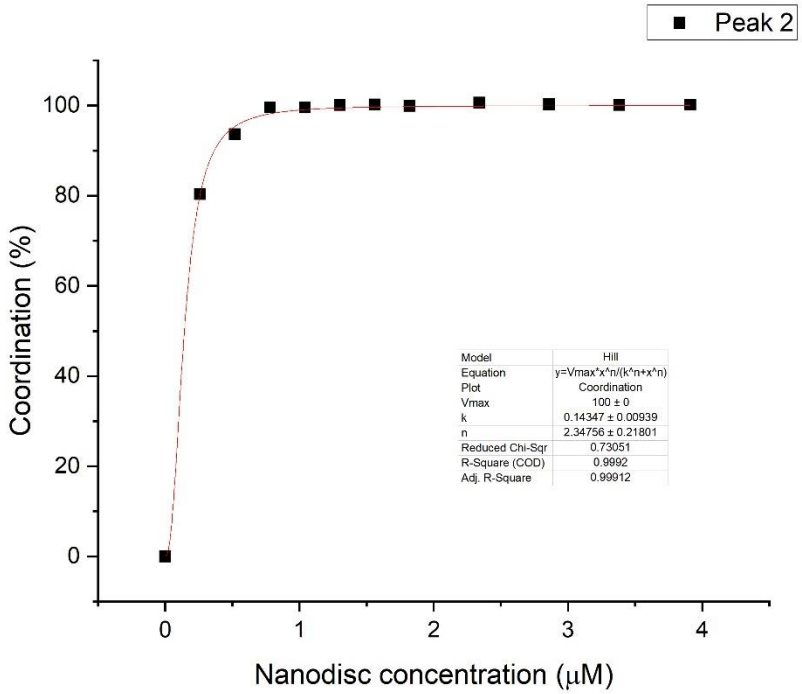

Figure S60 - Graph showing the percentage of **3**, peak b/2 coordinated to NCTC 13437 nanodiscs, with respect to increasing nanodisc concentration. Data was then fitted to the Hill Plot model with V_{max} fixed at 100 %.

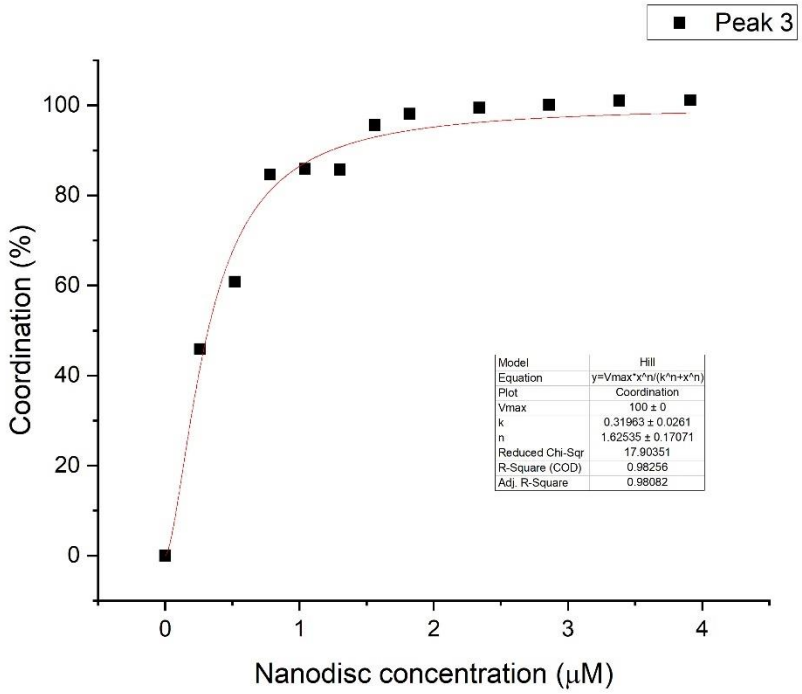

Figure S61 - Graph showing the percentage of **3**, peak c/3 coordinated to NCTC 13437 nanodiscs, with respect to increasing nanodisc concentration. Data was then fitted to the Hill Plot model with V_{max} fixed at 100 %.

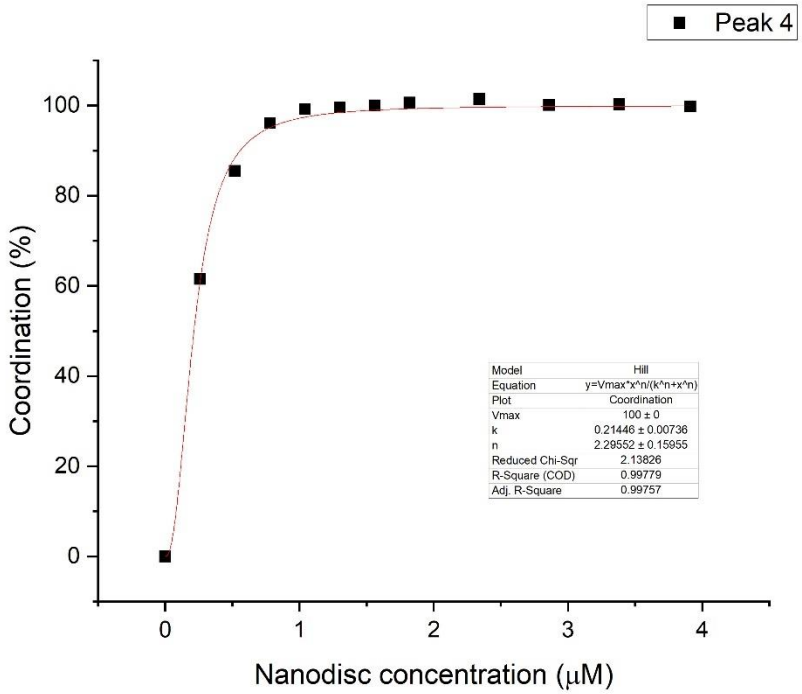

Figure S62 - Graph showing the percentage of **3**, peak d/4 coordinated to NCTC 13437 nanodiscs, with respect to increasing nanodisc concentration. Data was then fitted to the Hill Plot model with V_{max} fixed at 100 %.

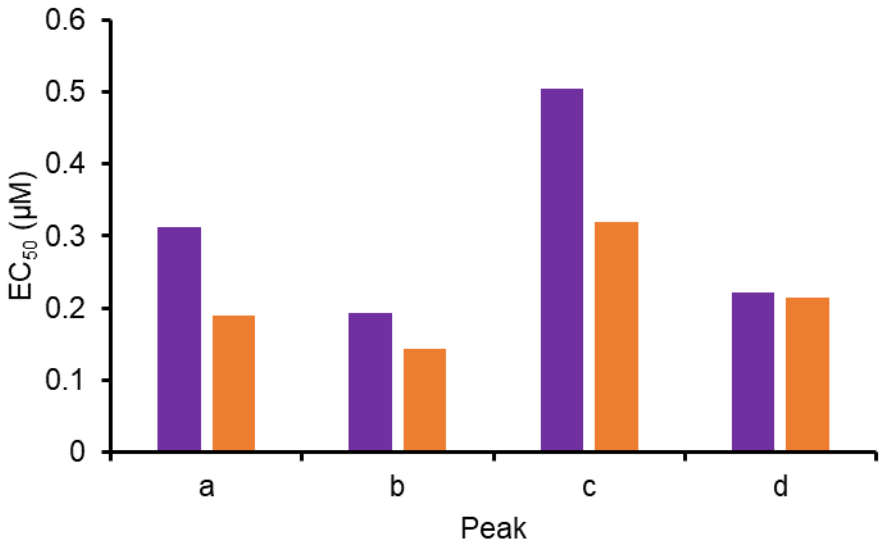

Figure S63 - EC_{50} (μM) values obtained from the fitting of peaks a – d of **3** titration data to Hill Plot kinetics using Origin 2018 software, with V_{max} fixed to 100 % of **3** bound to the nanodisc. Purple = results from PAO1 nanodiscs, orange = results from NCTC 13437 nanodiscs.

Section 10: Fluidity assay data

The results of membrane fluidity experiments conducted with phospholipid mixtures obtained from PAO1 and NCTC 13437 membranes did not show any changes in fluidity upon increasing concentrations of **1** – **3** at concentrations comparable to those used to conduct the previously discussed ^{1}H NMR nanodisc titration experiments.

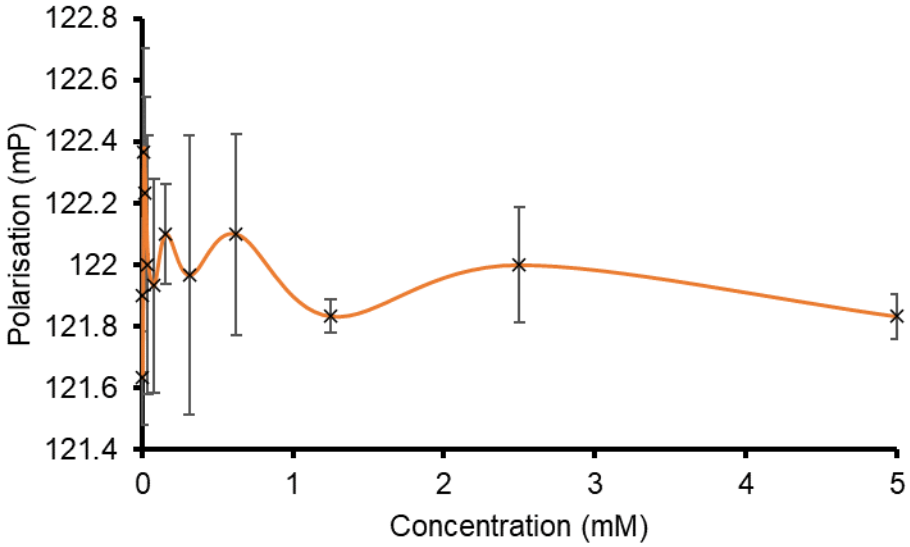

Figure S64 - Effect of **1** on FP measured in DPH labelled PAO1 vesicles at 25 ^{o}C. A target FP value of 100 mP was set to the DPH labelled vesicles.

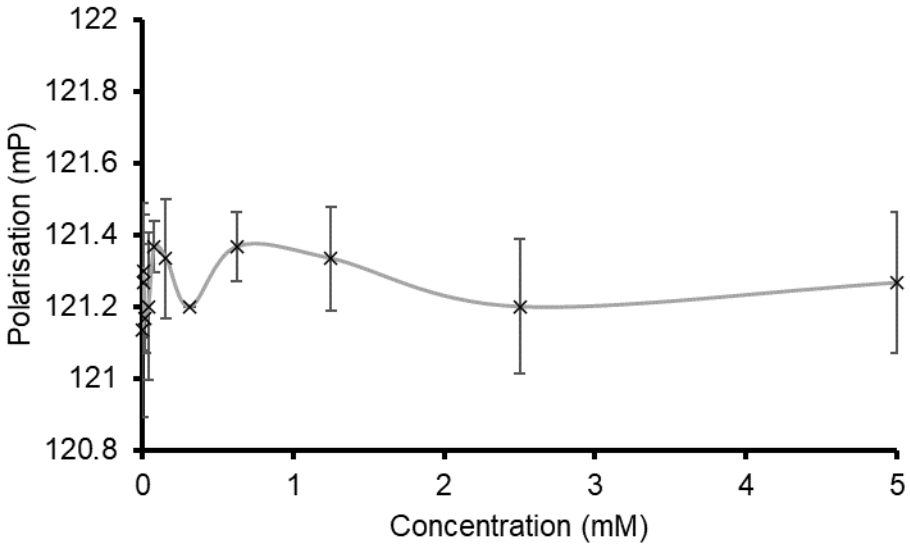

Figure S65 - Effect of **2** on FP measured in DPH labelled PAO1 vesicles at 25 ^{o}C. A target FP value of 100 mP was set to the DPH labelled vesicles.

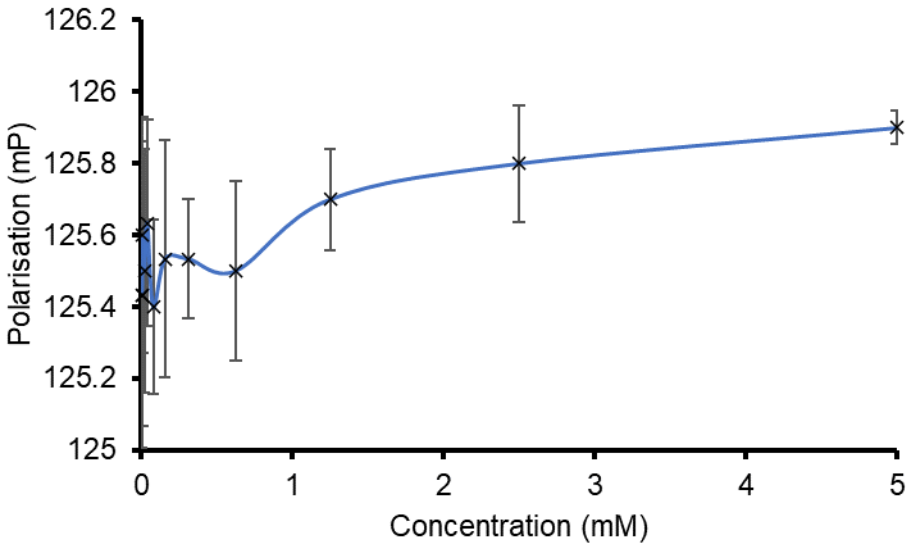

Figure S66 - Effect of **3** on FP measured in DPH labelled PAO1 vesicles at 25 °C. A target FP value of 100 mP was set to the DPH labelled vesicles.

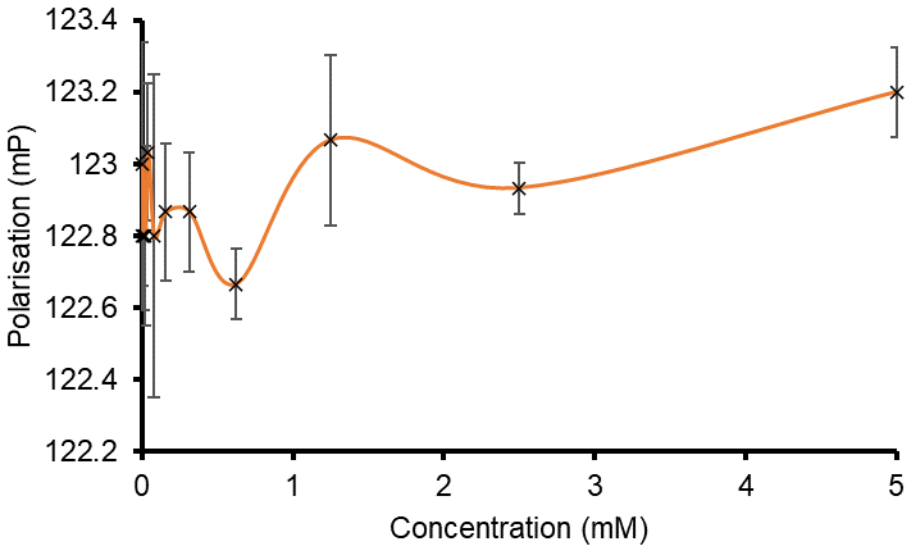

Figure S67 - Effect of **1** on FP measured in DPH labelled NCTC 13437 vesicles at 25 °C. A target FP value of 100 mP was set to the DPH labelled vesicles.

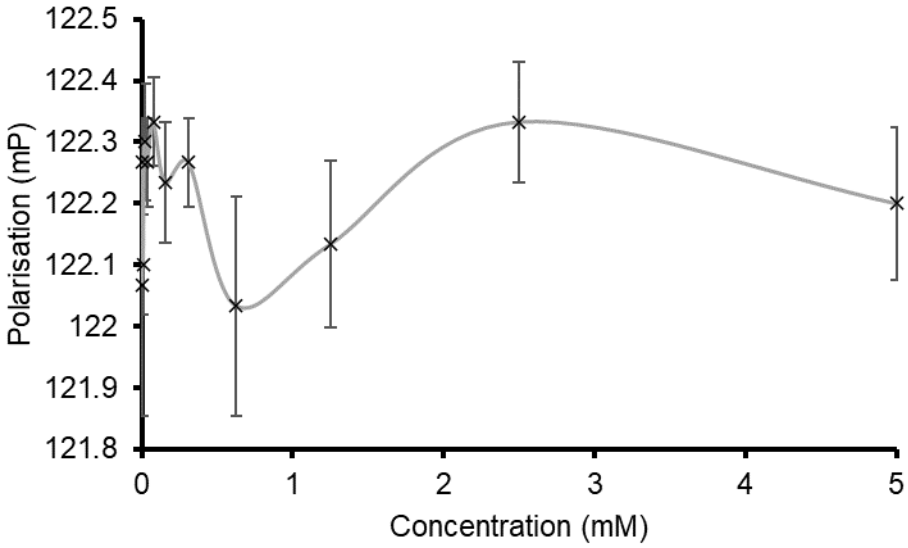

Figure S68 - Effect of **2** on FP measured in DPH labelled NCTC 13437 vesicles at 25 ºC. A target FP value of 100 mP was set to the DPH labelled vesicles.

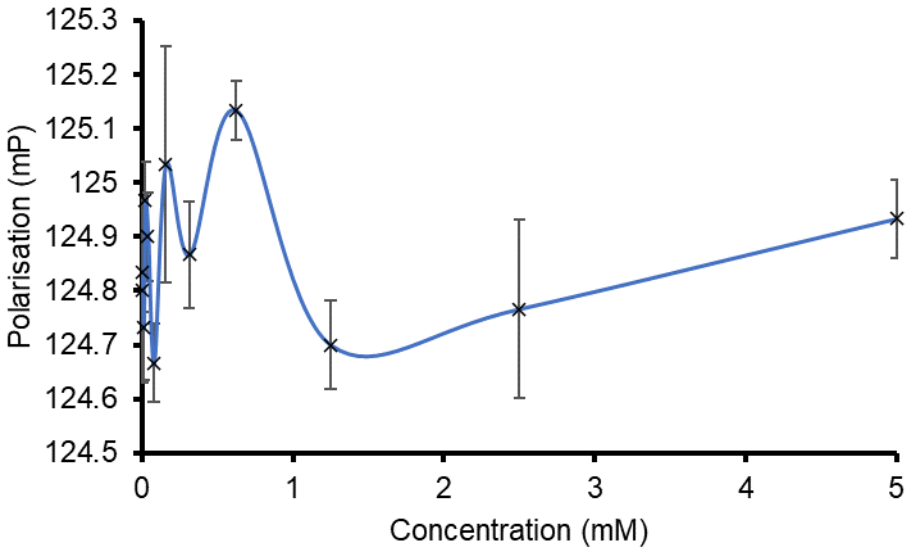

Figure S69 - Effect of **3** on FP measured in DPH labelled NCTC 13437 vesicles at 25 ºC. A target FP value of 100 mP was set to the DPH labelled vesicles.

Section 11: Minimum inhibitory concentration (MIC) data

Table S5 – Comparison between 50 % growth inhibition (MIC_{50}) and total growth inhibition (MIC).

	MIC (mM)			MIC_{50} (mM)		
Strain	**1**	**2**	**3**	**1**	**2**	**3**
PAO1 WT	12.5	>100	100	3.12	1.56-50	0.4
NCTC 13437	50	>100	100	6.25	0.4	0.8

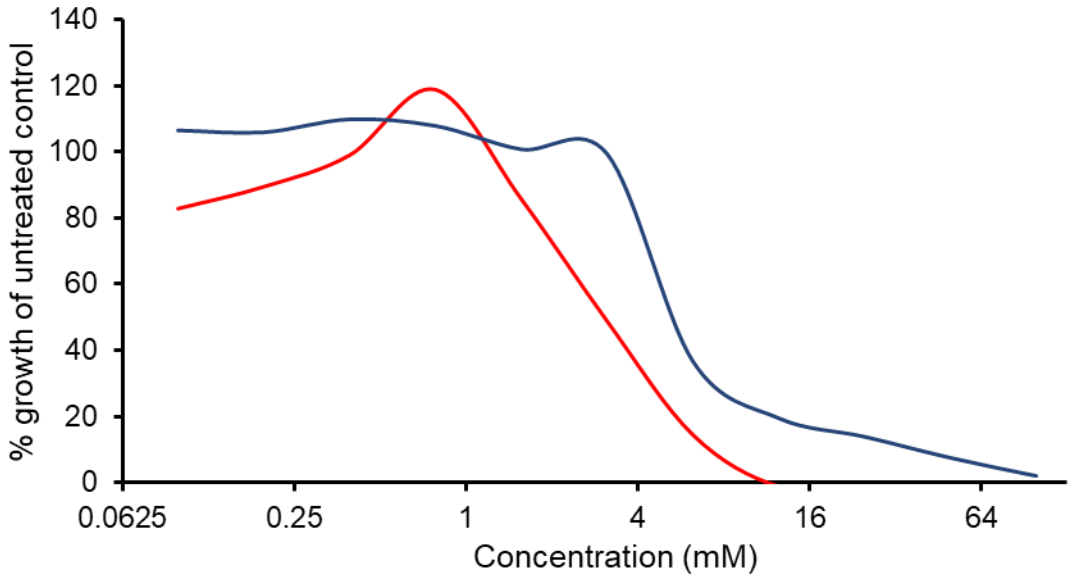

Figure S70 – End point values of **1** against *P. aeruginosa* strains. Red = PAO1, dark blue = NCTC 13437.

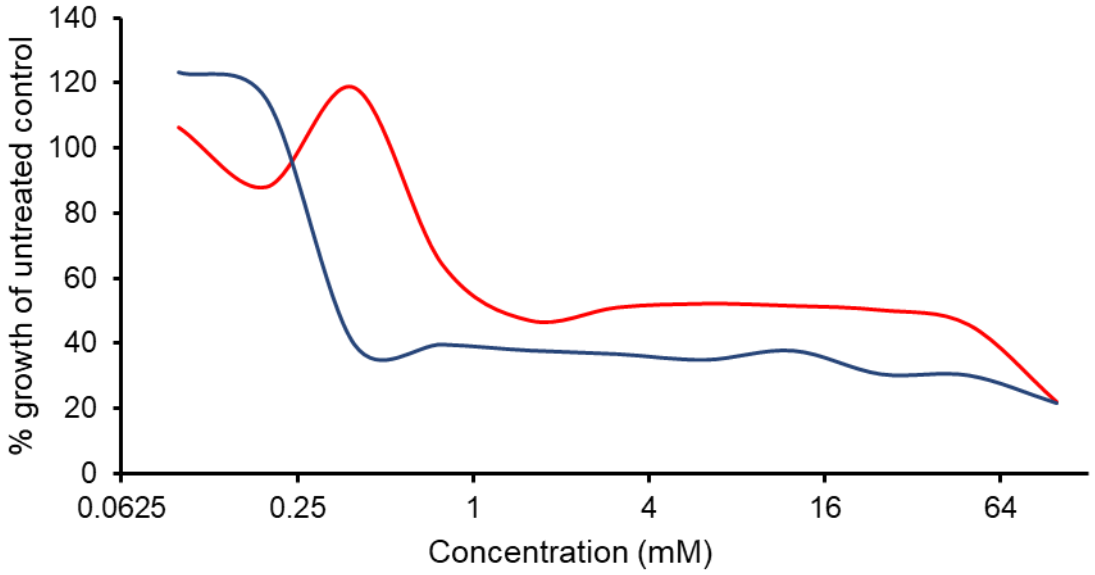

Figure S71 – End point values of **2** against *P. aeruginosa* strains. Red = PAO1 WT, dark blue = NCTC 13437.

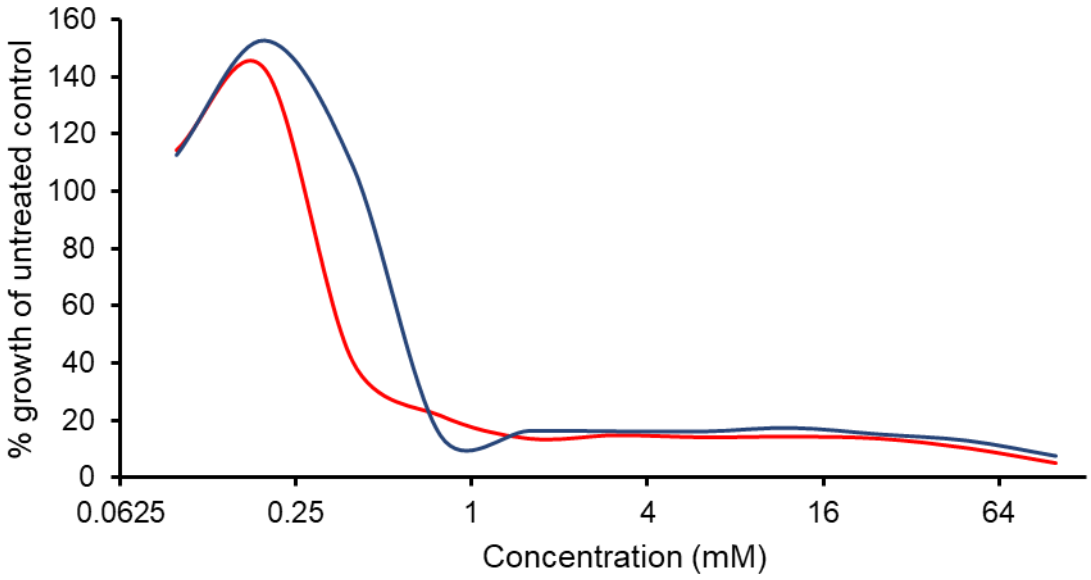

Figure S72 – End point values of **3** against *P. aeruginosa* strains. Red = PAO1 WT, dark blue = NCTC 13437.

Section 12: Scanning electron microscopy (SEM) data

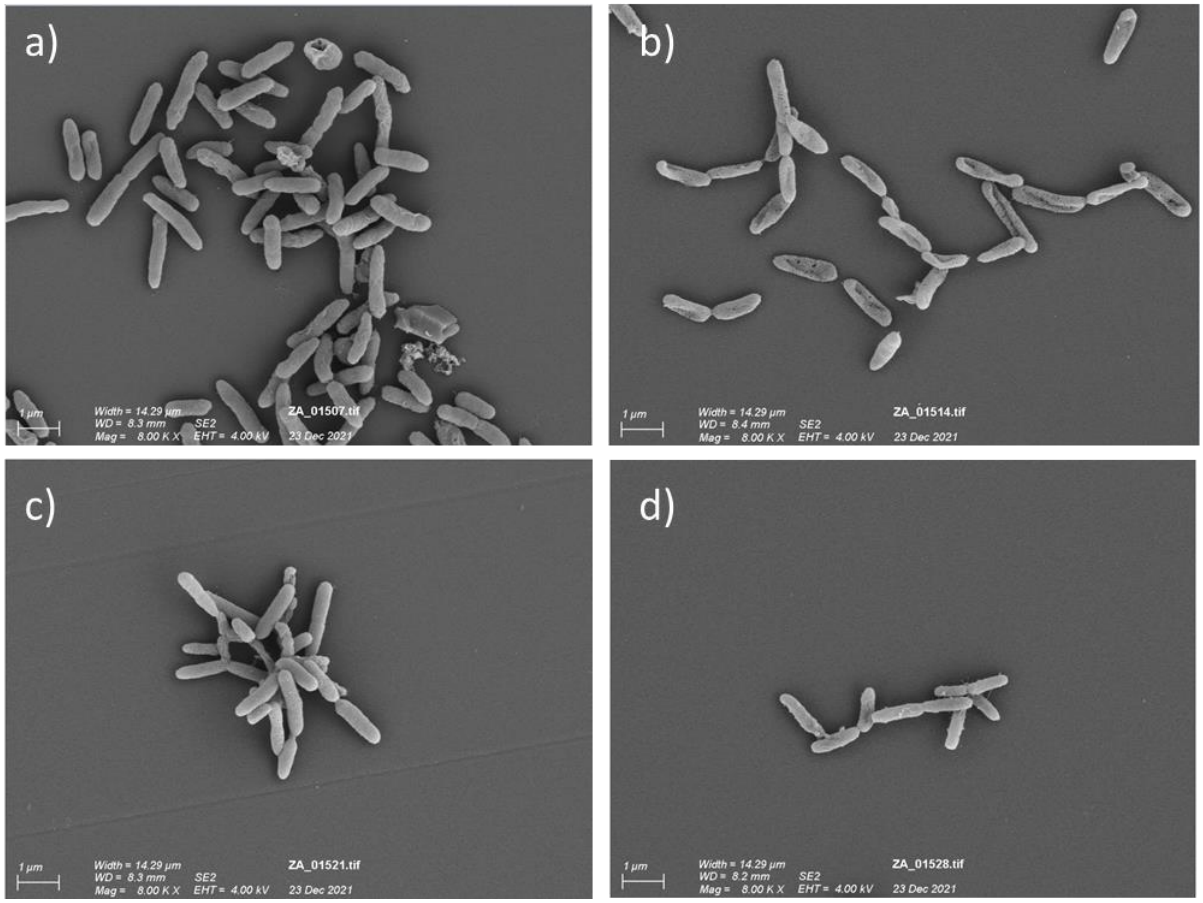

Figure S73 - Scanning electron microscopy of NCTC 13437 either untreated (a) or treated with 32mM of **1** (b), **2** (c) and **3** (d).

Section 14: References

1 J. Folch, M. Lees and G. H. Sloane Stanley, *J Biol Chem*, 1957, **226**, 497–509.
2 G. Townshend, G. S. Thompson, L. J. White, J. R. Hiscock and J. L. Ortega-Roldan, *Chem. Comm.*, 2020, **56**, 4015–4018.
3 H. Y. Carr and E. M. Purcell, *Phys. Rev.*, 1954, **94**, 630–638.
4 S. Meiboom and D. Gill, *Review of Scientific Instruments*, 1958, **29**, 688–691.
5 B. Luy and J. P. Marino, *J. Am. Chem. Soc.*, 2001, **123**, 11306–11307.
6 I. M. Helander and T. Mattila-Sandholm, *J Appl Microbiol*, 2000, **88**, 213–219.
7 A. Chattopadhyay and K. g. Harikumar, *FEBS Letters*, 1996, **391**, 199–202.
8 J. Wang, O. Morales-Collazo and A. Wei, *ACS Omega*, 2017, **2**, 1287–1294.
9 M. G. D'Andrea, C. C. Domingues, S. V. P. Malheiros, F. G. Neto, L. R. S. Barbosa, R. Itri, F. C. L. Almeida, E. de Paula and M. L. Bianconi, *Langmuir*, 2011, **27**, 8248–8256.
10 P. Di Profio, R. Germani, A. Fontana and V. Canale, *Journal of Molecular Liquids*, 2019, **278**, 650–657.